A Geochemical Analysis of Aluminum Hydroxides and Iron Oxides in Little Backbone Creek, Shasta County, California

Lauren C. Andrews
Senior Integrative Exercise
March 9, 2007

Submitted in partial fulfillment of the requirements for a Bachelor of Arts Degree from Carleton College, Northfield, Minnesota

Table of Contents

Abstract

Introduction……..1

Geologic Setting……4
Site Location *4*
Stratigraphy *4*
Balakala Rhyolite and Ore Bodies *5*

Mining History……..6

Remediation History…….....8

Methods…….....8
Field Parameters *11*
Water Samples *11*
Geochemical Modeling *12*
Precipitate Samples *13*
X-ray Diffraction and Scanning Electron Microscope *13*

Sources of Error……..…….14

Results……...15

Discussion…….28
Characterization of Iron Oxides *28*
Characterization of Aluminum Hydroxides *31*
Characterization of Trace Precipitates *33*
Copper and Sulfate Adsorption *33*
Further Research *36*

Conclusions……..36

Acknowledgements……..37

References...……..38

Appendix 1……....42

A Geochemical Analysis of Aluminum Hydroxides and Iron Oxides in Little Backbone Creek, Shasta County, California

Lauren C. Andrews
Carleton College
Senior Integrative Exercise
March 9, 2007

Advisor:
Bereket Haileab, Carleton College

ABSTRACT

Acidic mine water from the Mammoth Mine, Shasta County, California, causes an enrichment of sulfate, iron, aluminum and other trace metal concentrations in several nearby streams. The mixing of acidic water from Mammoth Mine with neutral surface water from Little Backbone Creek results in the precipitation of aluminum hydroxides and iron oxides in the streambed. Geochemical models of Little Backbone Creek predict the precipitation of kaolinite and gibbsite in Little Backbone Creek between the inflow of the Blow Out Tributary and the E-470 Tributary. However, goethite and hematite are the main constituents in the precipitate below the confluence of the E-470 Tributary and Little Backbone Creek. XRD and SEM analysis of both precipitates confirm the results of the geochemical model and indicate that trace metal and sulfate adsorption occurs on the surface of aluminum hydroxides. Chemical analysis of the water of Little Backbone Creek indicates that the shift in mineral precipitation is caused by changes in pH and metal concentrations due to the influx of acidic tributaries with different chemical compositions.

Keywords: Shasta County California, acid mine drainage, precipitation, gibbsite, goethite

INTRODUCTION

When deposits of sulfide minerals are exposed to the ambient atmosphere, oxidation results in the production of sulfuric acid (Stumm and Morgan, 1996; Ranville et al., 2004). The increase in acidity causes surface waters to become enriched in sulfate, iron, aluminum, and trace metals (Wentz, 1974; Bowell and Bruce, 1995; Munk et al., 2002). The process of sulfide dissolution occurs naturally; however, the mining process often exacerbates this problem by exposing sulfide rich ore to ground and surface water. When acid mine drainage is free to flow into nearby streams causing a range of environmental problems that affect the health and well-being of plants, animals, and humans that live in the area (Kristofers, 1973; Potter, 1976).

The mixing of surface water and acid mine drainage enriched in dissolved metals results in the precipitation of aluminum hydroxides and iron oxides in streambeds and banks due to geochemical changes in water and neutralization of pH (Edraki et al., 2005; Munk and Faure, 2004; Espana et al., 2006; Murad and Rojik, 2005). The chemical composition and crystalline structure of these precipitates is dependent on age, pH, and other geochemical parameters (Murad and Rojik, 2003). Iron oxides follow a fairly consistent pattern of precipitation. Jarosite is often stable at a pH lower than 2.5, schwertmannite is the dominant phase between pH 2.8 and a pH above 4.5 often results in the precipitation of goethite or ferrihydrate (Bigham et al., 1996). Aluminum precipitates have a different pattern of formation. Precipitation of aluminum sulfates is common below a pH of 4.5, while aluminum hydroxides tend to be stable above a pH of 4.5 (Nordstrom and Ball, 1986).

The adsorption of trace metals and sulfate onto aluminum and iron precipitates is well documented in acidic streams (Munk et al., 2002; Ranville et al., 2004; Sidenko and Sherriff, 2005) Trace metal adsorption relies on a wide range of factors including pH, water temperature, presence of bacteria, and organic content (McKnight and Bencala, 1988; McKnight et al., 1992; Kawano and Tomita, 2001; Murad and Rojik, 2003; DaSilva, 2006).

Previous work by Munk et al. (2002) found precipitation of aluminum hydroxides in acidic water with a pH of 6.3. Experimental neutralization of stream water shows that lead, copper, zinc, and nickel are adsorbed with increasing pH, while sulfate adsorption decreases with an increasing pH. Munk et al. (2002) also conclude that trace metal sorption is aided by the presence of sulfate at low pH values. A later study by Ranville et al. (2004) confirms that both aluminum hydroxides and iron oxides result from the neutralization of acid mine drainage. Ranville et al. (2004) also concludes that though most trace metals were rapidly removed from the system, changes in ambient conditions can result in the desorption of trace metals from the precipitates. Work by McKnight et al. (1988) and Gammons et al. (2005) expands the knowledge of the chemical behavior of acid mine drainage precipitates by examining the possibility of diel variations in iron and trace metal precipitation and the role of organic substances in trace metal adsorption.

Little Backbone Creek Watershed, Shasta County California, (Figure 1) provides an opportunity to study the impact of acid mine drainage from Mammoth Mine on a relatively uncontaminated stream and to examine the processes relating to the precipitation of both aluminum hydroxides and iron oxides. This study uses X-ray

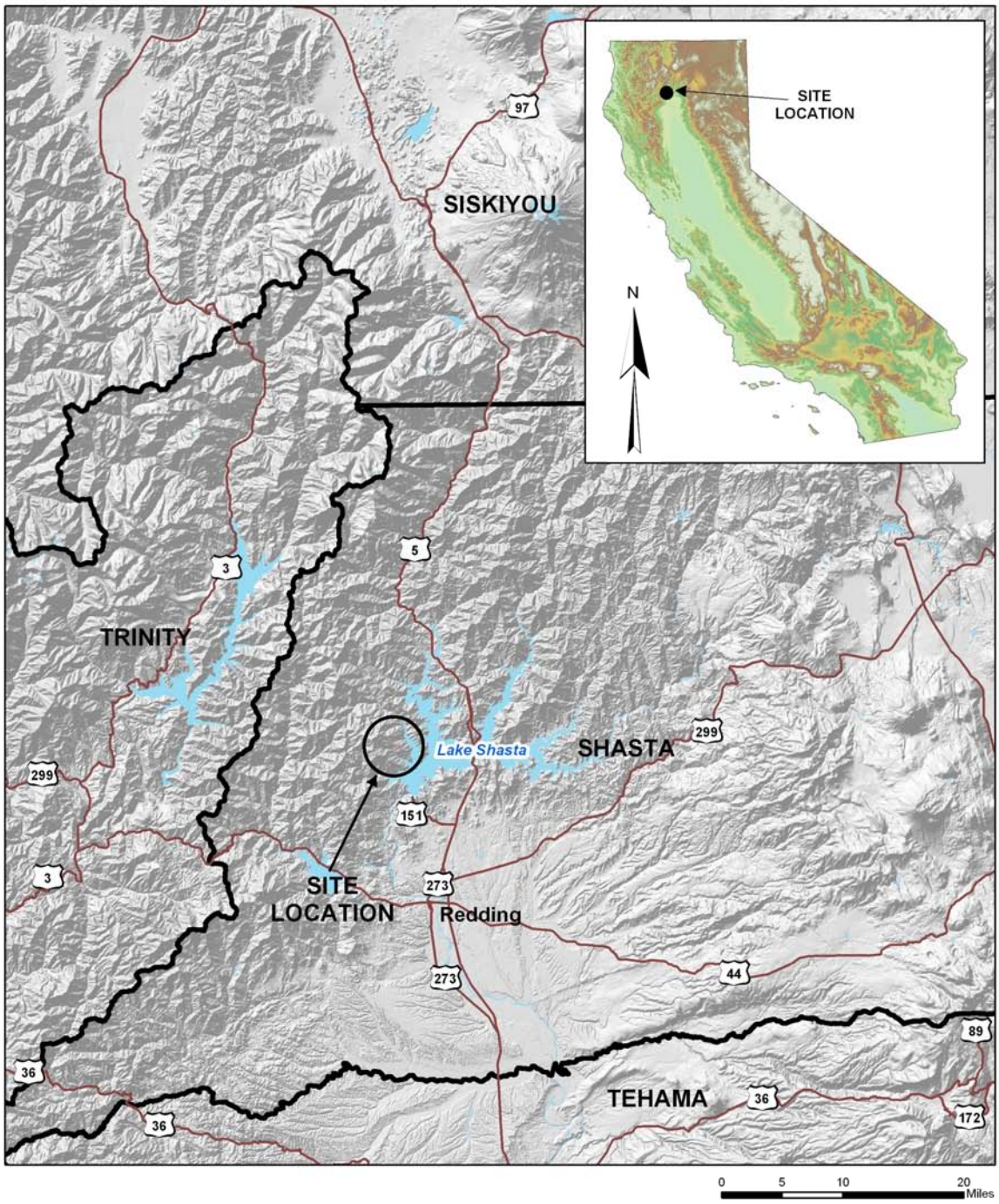

Figure 1. Little Backbone Creek is located on the northwestern side of Lake Shasta, Shasta County, California.

diffraction (XRD) and a scanning electron microscope (SEM) to analyze the chemical composition of both aluminum and iron precipitates. Geochemical modeling results are used to confirm mineral composition and characterize the geochemical relationship between precipitates and water of Little Backbone Creek.

GEOLOGIC SETTING

Site Location

Little Backbone Creek and Mammoth Mine are located in western Shasta County, California (Figure 1). The Little Backbone Creek watershed drains approximately four square miles, and flows in a southwesterly direction into Lake Shasta. The terrain in the Little Backbone Creek watershed is rugged; few slopes are less than 35 degrees and slopes of 50 degrees are common. The soil profile is thin and discontinuous. Elevations range from approximately 1000 feet above mean sea level at the confluence of Little Backbone Creek with Lake Shasta to 4,450 feet above mean sea level at the highest point in the watershed (Kinkel and Hall, 1952).

Stratigraphy

The Mammoth Mine is part of the West Shasta Copper-Zinc District, located in western Shasta County, which is stratigraphically composed of Devonian to present day geologic formations, the oldest of which is the Copley Greenstone of Middle Devonian age (Kinkel and Hall, 1952). Middle Devonian Balakala Rhyolite comfortably overlies the Copely Greenstone and is the main source of massive sulfide deposits in the region. Middle Devonian Kennett Formation, composed of limestone and shale, and the

Mississippian Bragdon Formation, composed of shale and sandstone, overly the Balakala Rhyolite (Kinkel and Hall, 1952). The Jurassic Mule Mountain Stock and Shasta Bally Batholith intrude the Copely and may have a role in the hydrothermal formation of the massive sulfide deposits found in the Balakala Rhyolite (Kinkel and Hall, 1952).

Balakala Rhyolite and Ore Bodies

Kinkel and Hall (1952) classified four different lithologies of the Balakala Rhyolite. Approximately 25 percent of the Balakala is interbedded flows of pyroclastic rocks that occur throughout the formation. The rest of the formation is composed of felsic sodic rhyolites with similar geochemistry and mineralogy but different lithologies. There is a large amount of interbedding in the transition between layers and pyroclastic flows that are seen throughout the formation. The oldest layer is nonporyphoritc with quartz phenocrysts smaller than 1millimeter (mm) with some mafic flows related to the underlying Copley Greenstone. The middle section has characteristic 1 to 4 mm quartz and feldspar phenocrysts that compose approximately 10 to 20 percent of the layer and an aphanitic groundmass. The youngest section of the Balakala Rhyolite is similar in appearance to the middle section; however, quartz and albite phenocrysts are greater than 4 mm in diameter. In addition, the Balakala Rhyolite exhibits thin, lenticular tuff beds and pyroclastic flows that are seen throughout the formation, but are concentrated in the middle layer. Both the tuff beds and the pyroclastic flows have chemistry similar to the rhyolitic flows (Kinkel and Hall, 1952).

The massive sulfide deposits that yield the ore removed from the West Shasta Copper-Zinc District are located in the upper middle section of the Balakala where phaneritic

rhyolite is overlain by pyroclastic flows (Kinkel et al., 1956) (Figure 2). The massive sulfide deposits were formed through hydrothermal replacement, most likely during the intrusion of several magmatic bodies including the Shasta Bally Batholith. The Mammoth Mine ore zone lies along the crest of a broad arch, and individual ore bodies are large, flat-lying, tabular bodies of copper and zinc-bearing pyritic ore (Kinkel and Hall, 1952). The massive sulfide deposits are composed of 60-98% ore and contain mainly pyrite, chalcopyrite and spalerite with minor amounts of magnetite, galena, tetrahedrite and pyrrhotite. Associated minerals include quartz, sericite and calcite (Kinkel et al., 1956).

MINING HISTORY

Mining in the West Shasta Copper-Zinc District began in the late 1800's. The Mammoth Mine, in particular, began production in 1905 and operated continuously until it was closed in 1919 due environmental problems associated with the copper smelting process (Kristofers, 1973). It was reopened briefly in 1923, but operations were halted permanently in 1925 (Kinkel and Hall, 1952; Kristofers, 1973). The Mammoth Mine was developed with thousands of feet of workings connected to several principal adits between the 200-foot (elevation of 941 meters) and 870-foot (elevation of 739 meters) levels (Kinkel and Hall, 1952).

Initially the ore was smelted for copper associated with chalcopyrite and the small amounts of gold; however, during World War I zinc prices were high enough to make zinc extraction profitable (Kristofers, 1973). Between 1905 and 1925, Mammoth Mine extracted 3,311,145 tons of ore that contained approximately 4% copper, 4.2% zinc, and 34.3% iron (Kristofers, 1973).

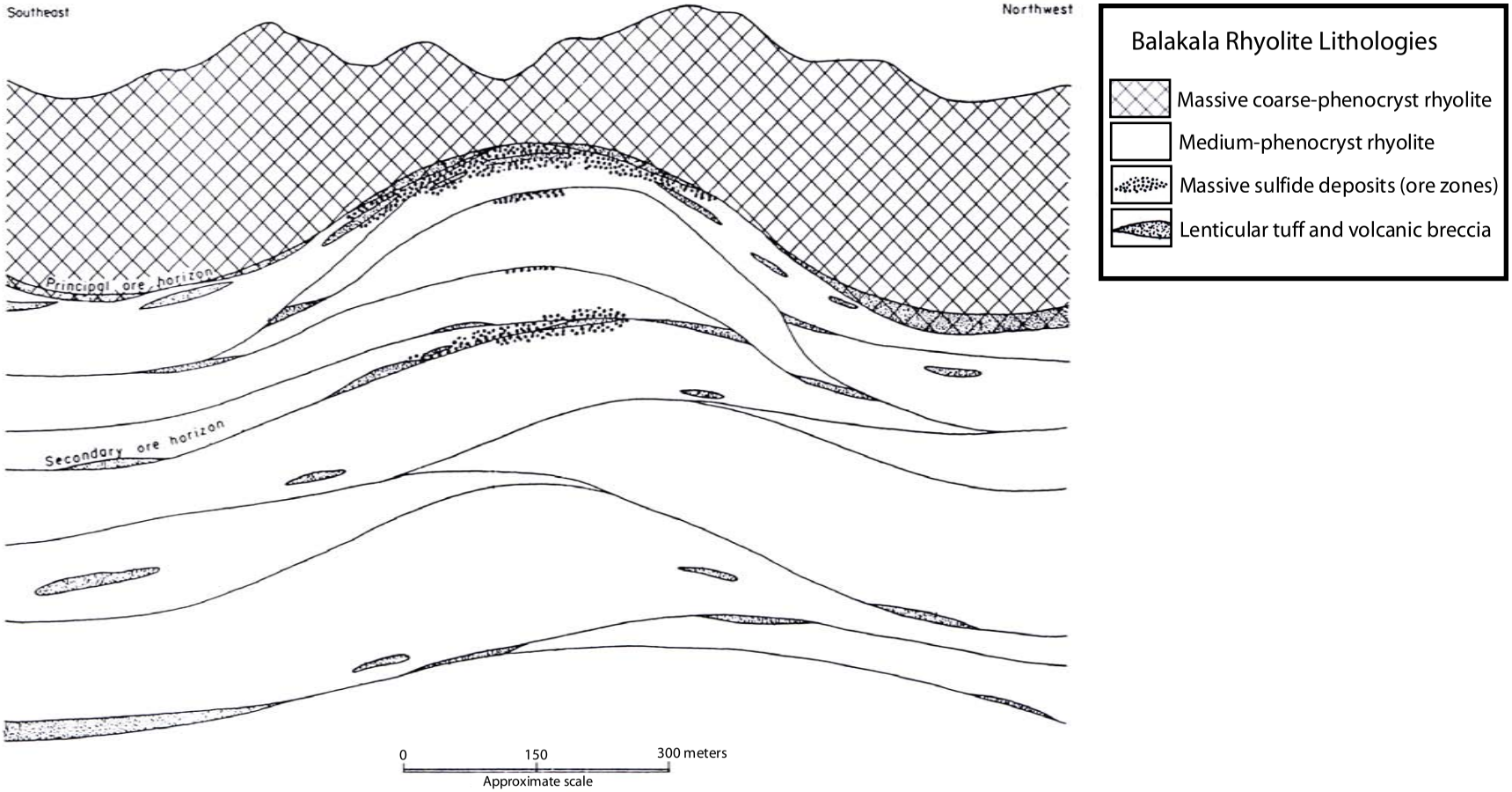

Figure 2. Massive sulifde deposit locations of the Mammoth Mine showing the relationship between Balakala rhyolite lithologies and the ore zones. Massive sulfide deposits at the Mammoth Mine are found in the fold hinge, primarily in the transition zone between the massive phenocryst rhyolite and mediumphenocryst rhyolite. Adapted from Kinkel and Hall (1952).

REMEDIATION HISTORY

Nine bulkhead seals were installed to reduce acid mine drainage from the main portals during the 1980's and early 1990's (VESTRA, 2005). Road maintenance, grading of several waste rock piles, and minor surface water controls are the only remedial activities that have been conducted in recent years (VESTRA, 2005). In the last two years, the watershed has become the focus for additional remediation to reduce metal loading to Lake Shasta.

METHODS

The sample locations in Little Backbone Creek were determined using a combination of established sample locations and examining areas of the stream that were most likely to demonstrate rapid change in the water chemistry. Basic geochemical field parameters were collected from 12 locations, water samples were collected from eight locations, and rock samples were collected from seven locations along Little Backbone Creek (Figure 3; Table 1). The remote location of Little Backbone Creek required that all the sampling equipment be carried to the sample locations and all water and rock samples had to be carried out precluding a more extensive sampling plan.

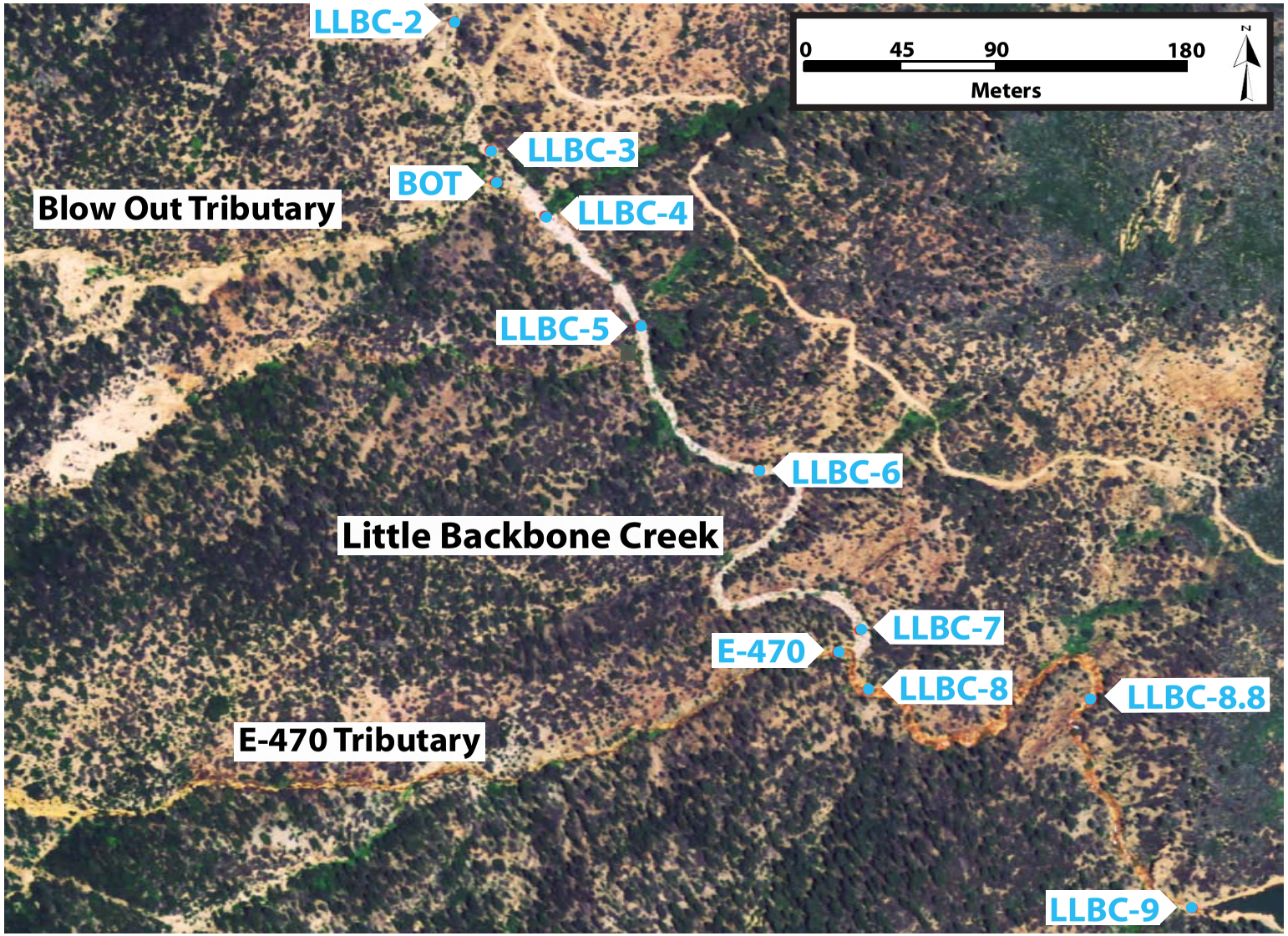

Figure 3. Sample locations are labeled in blue, while Little Backbone Creek and tributaries are labeled in black. The Mammoth Mine portal, E-470 portal, and associated tailings piles are to the west of Little Backbone Creek.

TABLE 1. TYPE OF SAMPLE AT EACH LOCATION

Sample Location	LLBC-2	LLBC-3	BOT	LLBC-4	LLBC-5	LLBC-6	LLBC-7	E-470 Trib.	LLBC-8	LLBC-8.8	LLBC-9	E-470 Portal
Photograph	●	●	●	●	●	●	●	●	●	●	●	●
GPS	●	●	●	●	●	●	●	●	●	●	●	●
Field Parameters	●	●	●	●	●	●	●	●	●	●	●	●
Water Sample		●	●	●			●	●	●		●	●
Precipitate Sample		●		●		●	●		●	●	●	

Field Parameters

All instruments and containers used to measure field parameters were rinsed with distilled water and stream water from the sample location. Parameters were collected from areas that displayed predominant conditions for the given sample location. Dissolved oxygen was measured with the YSI 550A dissolved oxygen meter and temperature was recorded using associated digital thermometer directly from Little Backbone Creek. Oxidation- reduction potential was measured with the EUTECH instruments OPR Tester and electrical conductivity and pH were measured with Hanna Instruments HI 98311 and HI 98127 in a beaker of collected water. Acidity and alkalinity were measured using field test kits, the Hach AC-6 low range acidity test and the LaMotte Wat-DR Alkalinity test kit, respectively.

Flow measurements for the past year were furnished by Mining Remedial Recovery Company. Flow measurements on the days of sampling were collected using a FP 101 Global Flow Probe water velocity meter every 4 inches along a transect. Stream depth and measurements collected using the water velocity meter were used to calculate the average flow of the stream at each sample location.

Water Samples

Water samples were taken at eight locations associated with field parameters along Little Backbone Creek. All samples were collected near the middle of the stream where flow conditions were most uniform and characteristic for the sample location. The unfiltered samples for cations (calcium, magnesium, potassium, sodium, and silicon) and alkalinity were collected in a polyurethane bottle. Chloride, sulfate and nitrate samples

were filtered in the field using a Nalgene hand pump filter and collected in a polyurethane bottle. Dissolved metals including aluminum, zinc, copper and iron were filtered following the above procedure and preserved in with 1:1 molar nitric acid in order to prevent metal precipitation. Total iron was preserved in 1:1 molar nitric acid. All samples were preserved by lowering their temperature to approximately 4 degrees Celsius upon completing all sampling procedures. A field duplicate was taken at LLBC-4, following all of the above water sampling procedures. Samples were analyzed by Basic Laboratories, Redding, CA, using standard methods as determined by the California Environmental Protection Agency.

Geochemical Modeling

In order to theoretically identify the precipitates in Little Backbone Creek, saturation indices were calculated using the PHREEQC geochemical modeling program (Parkhurst, 1999). PHREEQC determines the saturation index of a mineral by relating the ion activity product (IAP) observed in solution and the theoretical solubility product (Ksp) using the equation SI=Log (IAP/Ksp) (Parkhurst, 1999). Saturation indices can be simply defined as the concentration at which dissolved concentrations of mineral components are saturation with respect to the conditions of the solution. If the saturation index of the solution is greater than zero then the solution is supersaturated with respect to the solid form of the mineral and precipitation with theoretically occur. If the saturation index is less than zero then the solution is understaturated with respect to the mineral and dissolution theoretically occurs. A saturation index equal to zero indicates that the solid

and the solution are in equilibrium with respect to a mineral. Chemical results from water sample analysis were used as parameters for the geochemical modeling.

Precipitate Samples

Rock samples were collected at seven locations associated with field parameters along Little Backbone Creek. Rocks within a 10 foot radius of the sample location were examined for precipitate. Though all rocks were covered with either a red or white precipitate, only rocks with sufficient precipitate were collected and placed in plastic bags. After collection, each rock sample was gently scraped with a nylon toothbrush and sorted to remove particles not associated with the precipitate. Only five rock samples yielded enough precipitate for XRD and SEM analysis.

X-ray Diffraction and Scanning Electron Microscope

Precipitate XRD patterns were obtained using a Philips PW1877 X-ray Diffractometer maintained by the Carleton College Department of Geology. The precipitate was disaggregated in with a mortar and pestle and dissolved in approximately 0.5 milliliters (mL) of distilled water. The precipitate was allowed to settle and clear water was decanted of the top of the mixture. The remaining mixture was placed on a glass slide mount using a pipette and then smeared to evenly cover the surface. Samples were scanned from 0° to 70° 2θ at 40kV and 55mA. Peaks were identified using published mineral d-spacing peaks.

The resulting precipitants were analyzed using the SEM owned by Carleton College. Samples were mounted on a carbon sheet and analyzed at 60 kV for percent weight of precipitate components and the presence of trace metals.

SOURCES OF ERROR

Though the XRD results displayed several significant peaks, peak measurements did not correspond precipitates related to waters affected by acid mine drainage. There are several sources of error that can be directly identified in the preparation, and analysis of the precipitates. In order to account for the possibility that such errors had affected XRD analysis a simple calculation of the possible errors was performed. In order to account for technical difficulties experienced while performing XRD analysis, the silicon standard was analyzed and the measured d-spacings were compared to accepted standards for the d-spacing of silicon. This comparison yielded approximately a ±0.1 error in d-spacing relative to accepted standards. This error was then taken into consideration when determining the identification of precipitates. Results from XRD analysis of the precipitate samples identified several minerals that corresponded to the results of both SEM and geochemical modeling data. All samples had d-spacings with the highest relative intensities correspond to the d-spacings of quartz due to the use of glass sample holders, but peaks with smaller relative intensities correspond to minerals seen in the precipitates.

SEM analysis was performed on a raw sample without carbon coating or sample orientation. Therefore, the data collected from the analysis can only be used in qualitative analysis of the precipitate.

RESULTS

The aluminum precipitate (Figure 4) extends from slightly above the confluence of the Blow Out Tributary and Little Backbone Creek to the confluence of the E-470 Tributary and Little Backbone Creek. The precipitate covers most of the rock surfaces completely and comes off easily when rubbed. There is accumulation of aluminum precipitate at LLBC-3; however, this mineral precipitation is minor in comparison with the mineral precipitation found below the entrance of the Blow Out Tributary. The iron precipitate covers most of the streambed surfaces from LLBC-8 to LLBC-9, but decreases in concentration downstream (Figure 5).

In contrast to Little Backbone Creek the Blow Out Tributary and the E-470 Tributary, do not show precipitation of aluminum hydroxides or iron oxides. The Blow Out Tributary is the first stream affected by acid mine drainage to enter Little Backbone Creek, between LLBC-3 and LLBC-4. The E-470 Tributary enters Little Backbone Creek between LLBC-7 and LLBC-8.

Field measurements show that there is a change in water geochemistry in Little Backbone Creek after the inflow of the Blow Out Tributary and the E-470 Tributary (Table 2). The most prominent change in water conditions is the drop in pH. At LLBC-3 the pH is approximately 6.3; however, pH decreases to 4.8 after the Blow Out Tributary enters Little Backbone Creek (Figure 6). After the initial influx of acid mine drainage

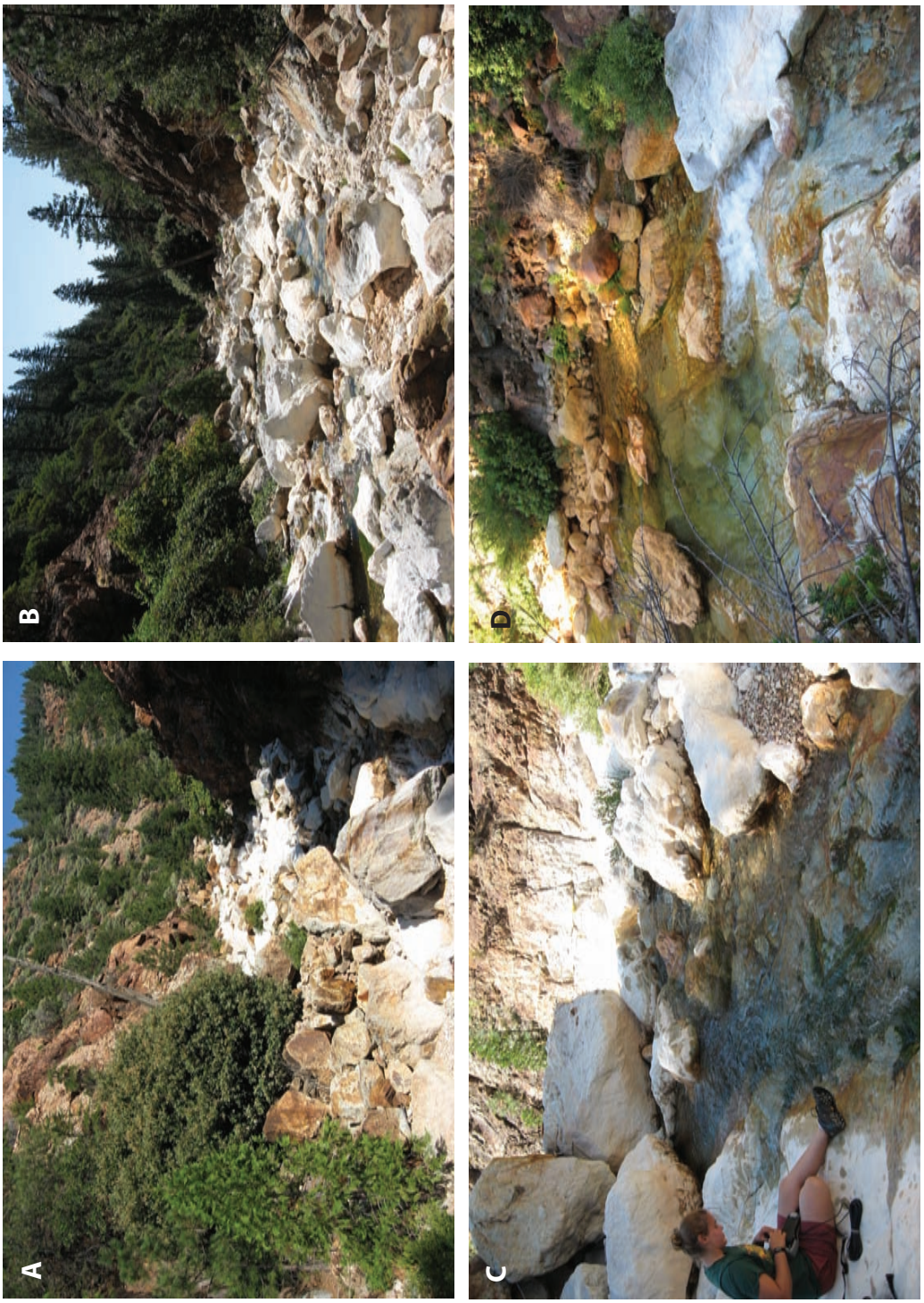

Figure 4. A) Sample location, LLBC-4. B) LLBC-5, near the entrance of the 5.1 Tributary. C) LLBC-7. D) The transition of precipitates at the entrance of the E-470 Tributary.

Figure 5. LLBC-8 is the site loction farthest upstream site displaying red precipitate. B) Precipitate between LLBC-8 and LLBC-8.8. C) Precipitate at LLBC-8.8. D) Decreased precipitation at LLBC-9 due to mixing with Lake Shasta.

TABLE 2. FIELD PARAMETER MEASUREMENTS

Site Location	LLBC-2	LLBC-3	BOT	LLBC-4	LLBC-5	LLBC-6	LLBC-7	E-470 Trib.	LLBC-8	LLBC-9	E-470 Portal
Flow (gal/m)	340	420	310	880	1100	1150	1280	25	1290	1580	NA
pH (pH units)	6.8	6.4	4.4	4.9	4.3	4.8	4.8	4.1	4.8	4.7	2.1
Dissolved oxygen (mg/L)	9.35	9.13	9.56	10.01	8.9	8.94	9.14	8.3	8.94	9.12	2.09
Electrical conductivity (µS)	80.4	87	588	356	358	344	346	521	355	358	3746
Oxidation-reduction (mV)	358	383	511	458	467	466	470	422	481	493	515
Alkalinity (mg/L)	4	4	0	5	0	0	0	0	0	0	0
Acidity (mg/L)	20	20	180	80	100	100	100	140	100	120	800
Water temperature (°C)	18.7	18.5	17.7	16.7	19.7	19.8	19.5	21.8	18.8	18.4	14
Air temperature (°C)	29.4	27.2	35	25.6	29.4	28.9	28.9	26.1	26.1	25	21.1
Downstream distance (m)	0	154	NA	240.03	388.62	588.645	974	NA	1040	1680	NA

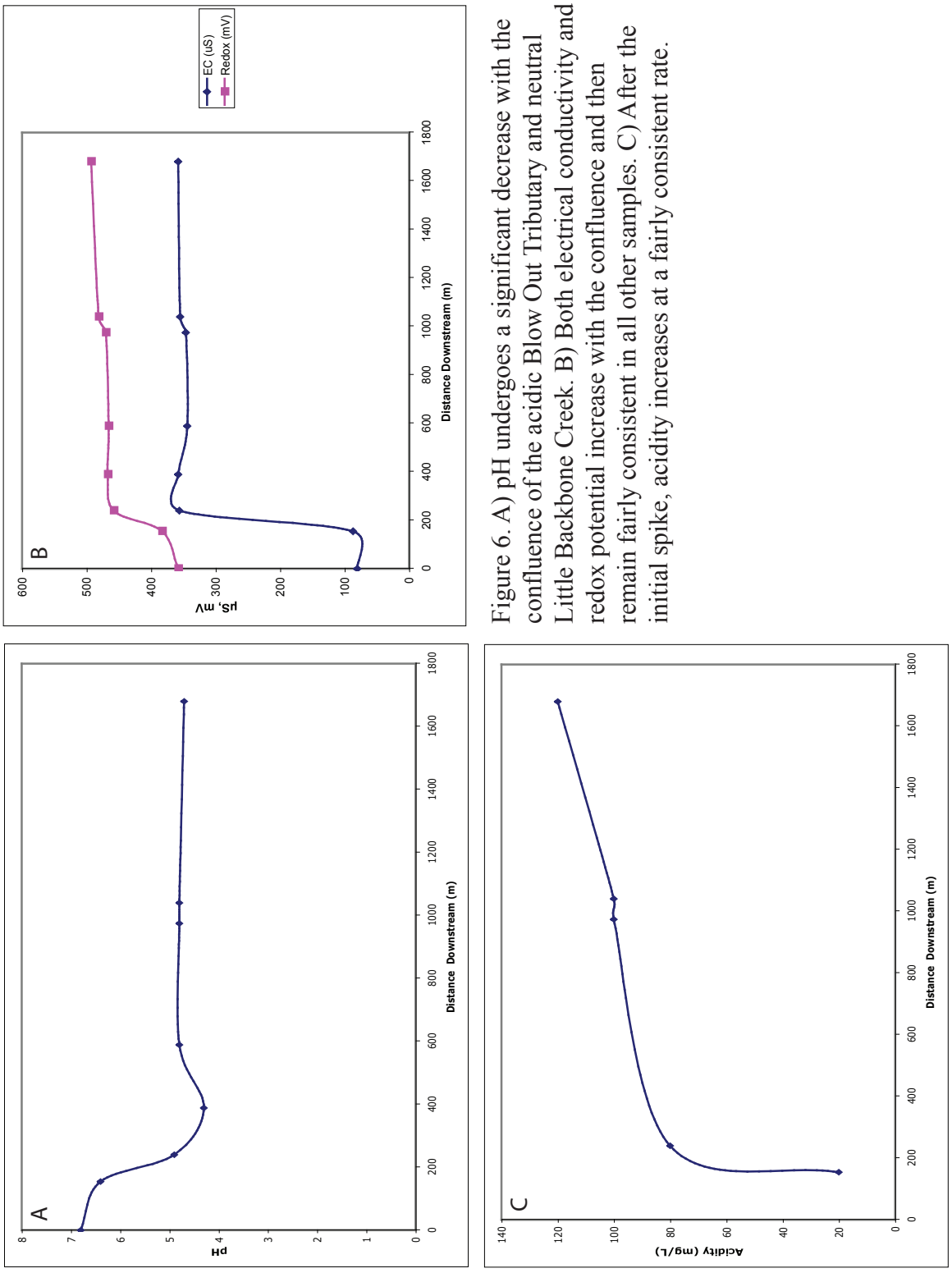

Figure 6. A) pH undergoes a significant decrease with the confluence of the acidic Blow Out Tributary and neutral Little Backbone Creek. B) Both electrical conductivity and redox potential increase with the confluence and then remain fairly consistent in all other samples. C) After the initial spike, acidity increases at a fairly consistent rate.

associated with the Blow Out Tributary, the pH remains fairly stable at the remainder of the sample locations in Little Backbone Creek.

Electrical conductivity and reduction-oxidation potential of the water in Little Backbone Creek increase at LLBC-4, after the mixing of Blow Out Tributary and Little Backbone Creek (Figure 6).

In addition, acidity concentrations increase and alkalinity concentrations decrease to zero as flow moves downstream (Figure 6; Table 3).

Water sample results are summarized in Table 3. The water sample from LLBC-3 has low concentrations of aluminum, zinc and copper, 33 micrograms per liter (µg/L), 247 µg/L and 58 µg/L, respectively. Dissolved aluminum, zinc, and copper concentrations increase significantly between LLBC-3 and LLBC-4 to 9820 µg/L, 3520 µg/L and 1770 µg/L, respectively. Between LLBC-4 and LLBC-7 aluminum, zinc, and copper concentrations decrease and then stabilize after LLBC-8 (Figure 7). In contrast, dissolved iron concentrations increase at a consistent rate from LLBC-4 and LLBC-7, and then experience a drastic increase between LLBC-7 and LLBC-8 followed by a decrease between LLBC-8 and LLBC-9 (Figure 7).

Concentrations of dissolved aluminum, zinc, copper and iron in water from the Blow Out Tributary are significantly higher than concentrations found in Little Backbone Creek (Table 3). The E-470 mine pool also has elevated concentrations of aluminum, zinc and, copper, but concentrations in the water at E-470 Tributary are below the concentrations found in Little Backbone Creek, while iron remains above levels found in Little Backbone Creek (Table 3).

TABLE 3. WATER GEOCHEMISTRY RESULTS

Analysis	LLBC-3	BOT	LLBC-4	LLBC-7	E-470 Trib.	LLBC-8	LLBC-9	E-470 Portal
Dissolved Metals ((µg/L))								
Aluminum	33	17200	9820	8680	7190	9110	8990	45400
Copper	58	3140	1770	1580	1340	1640	1630	27500
Iron	0	88	30	54	203	67	65	383000
Zinc	247	6320	3520	3220	3830	3260	3340	55300
Total Metals (mg/L)								
Iron	48	95	68	69	210	76	64	384000
Cations (mg/L)								
Calcium	5	45	26	25	33	26	26	109
Magnesium	2	13	8	8	13	8	8	38
Potassium	0	0.7	0.3	0.4	0	0.4	0.3	0.3
Silicon	8.31	15.5	12.5	11.7	14.5	11.7	11.9	32.1
Sodium	3	5	4	4	5	4	4	7
Anions (mg/L)								
Chloride	0.17	0	0.93	0	0	0	0	0
Nitrate	0.03	0.03	0.04	0.02	0	0.11	0.02	0.06
Sulfate	27.1	332	200	181	231	183	188	2310
Alkalinity	2	0	0	0	0	0	0	0
Bicarbonate	3	0	0	0	0	0	0	0

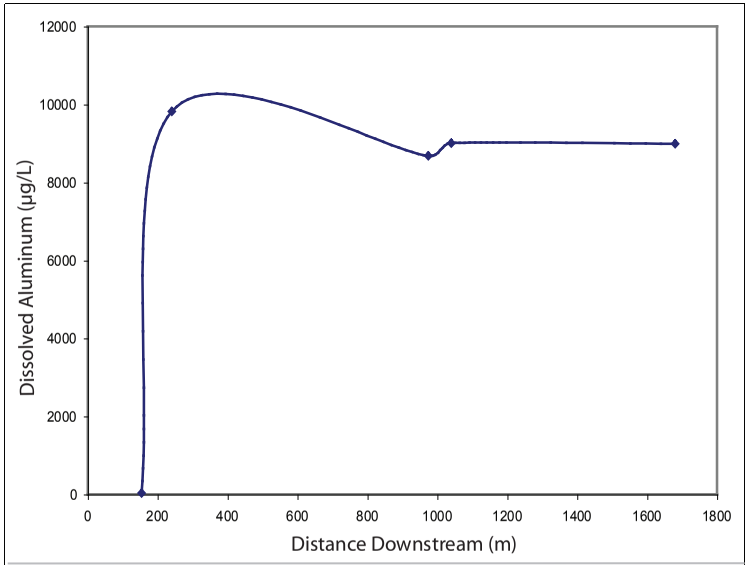

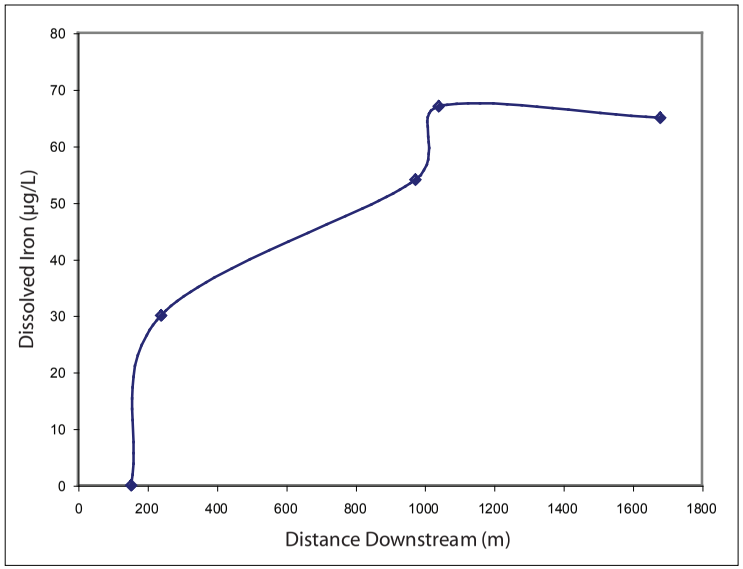

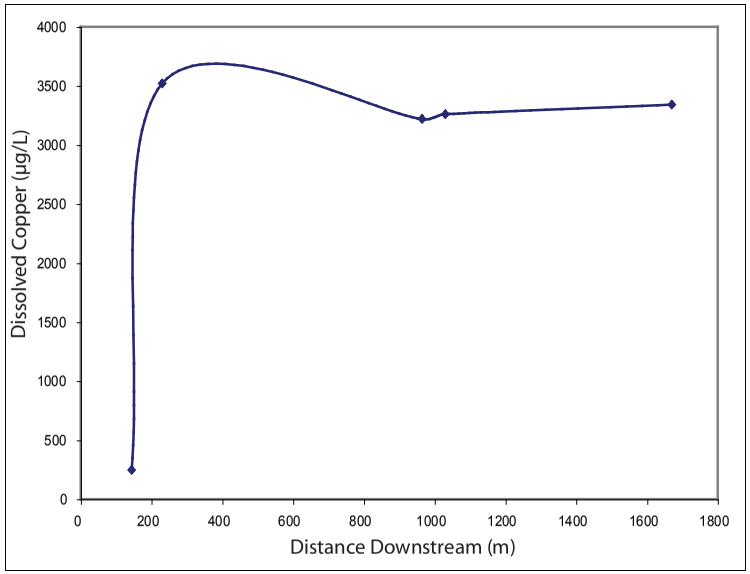

Figure 7. A, C, D) All dissolved metals experience an increase in concentration with the influx of the Blow Out Tributary. Aluminum, copper and zinc decrease between LLBC-4 and LLBC-7 as a result of the precipitation of aluminum hydroxides. After the influx of the E-470 Tributary these metals act in a relatively conservative manner. B) Dissolved iron continues to increase from LLBC-4 to LLBC-7. Between LLBC-7 and LLBC-8, the influx of the E-470 Tributary corresponds to a significant increase in iron concentrations, after which concentrations undergo a slight decrease.

Total iron initially increases between LLBC-3 and LLBC-4 then maintains a constant concentration between LLBC-4 and LLBC-7. There is a significant increase between LLBC-7 and LLBC-8 before a decrease between LLBC-8 and LLBC-9 (Figure 7).

The initial concentrations of magnesium, potassium, silicon, and sodium fall within a wide range, yet these concentrations all increase between LLBC-3 and LLBC-4 then behave in a conservative manner between LLBC-4 and LLBC-9 (Figure 8; Table 3). In contrast, calcium increases between LLBC-3 and LLBC-4, decreases from LLBC-4 to LLBC-7, and remains stable after LLBC-8.

The concentrations of cations from samples at the E-470 Portal, E-470 Tributary, and Blow Out Tributary are higher then concentrations measured at sample locations on Little Backbone Creek (Table 3).

Sulfate concentrations demonstrate an initial increase in concentration from LLBC-3 to LLBC-4 then concentrations begin to decrease between LLBC-4 and LLBC-7 then stabilize (Figure 9). Sulfate concentrations in both the tributaries and the E-470 Portal are above the concentrations in Little Backbone Creek. In contrast, nitrate concentrations are within a fairly small range except for a peak at LLBC-8 (Figure 9). LLBC-3 and LLBC-4 are the only sample locations at which chloride were detected, with concentrations of 0.17 milligrams per liter (mg/L) and 0.93 mg/L, respectively. LLBC-3 is the only sample location with detectable concentrations of alkalinity and bicarbonate; carbonate was undetectable at all sample locations (Table 3).

Geochemical modeling using water chemistry results indicates that LLBC-4, LLBC-7, LLBC-8, and LLBC-9 all have the tendency to precipitate the same minerals

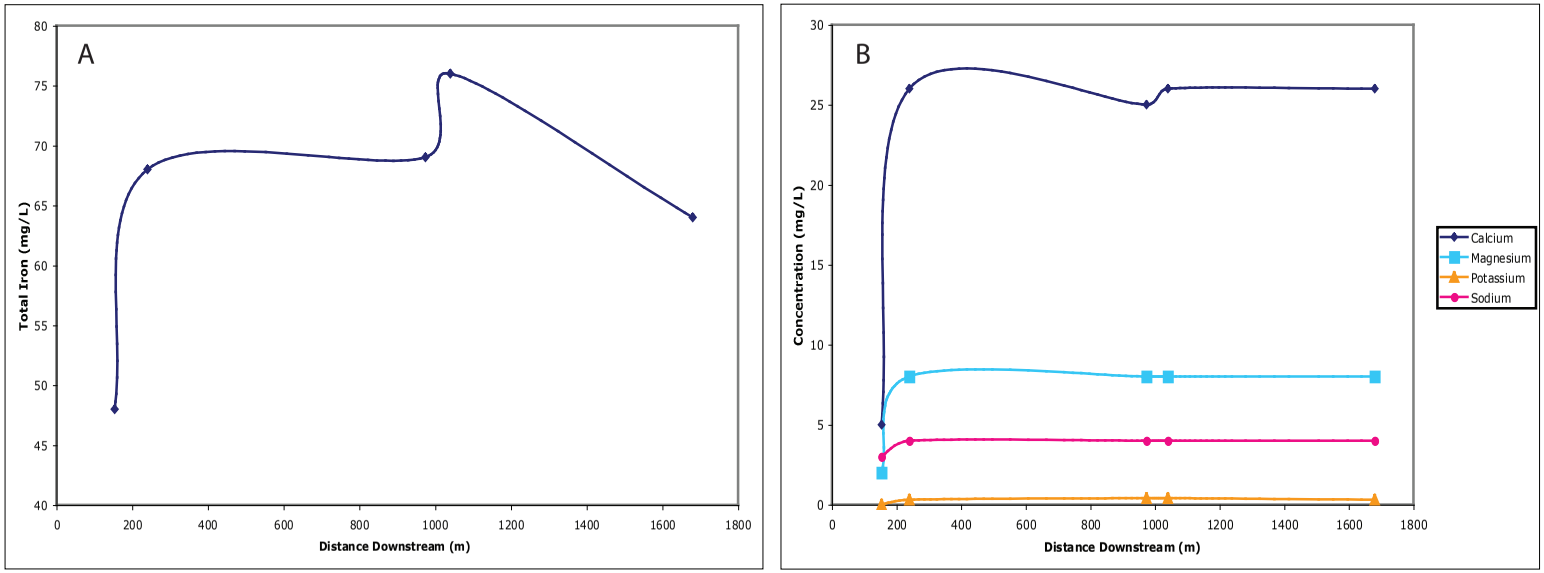

Figure 8. A) After the initial increase in the concentration, total iron remains constant. A second increase corresponds to the inflow of the E-470 Tributary, after which concentrations decrease as a results of the formation of iron oxide precipitates. B) Magnesium, calcium and silicon behave conservatively after the initial increase in concentration.

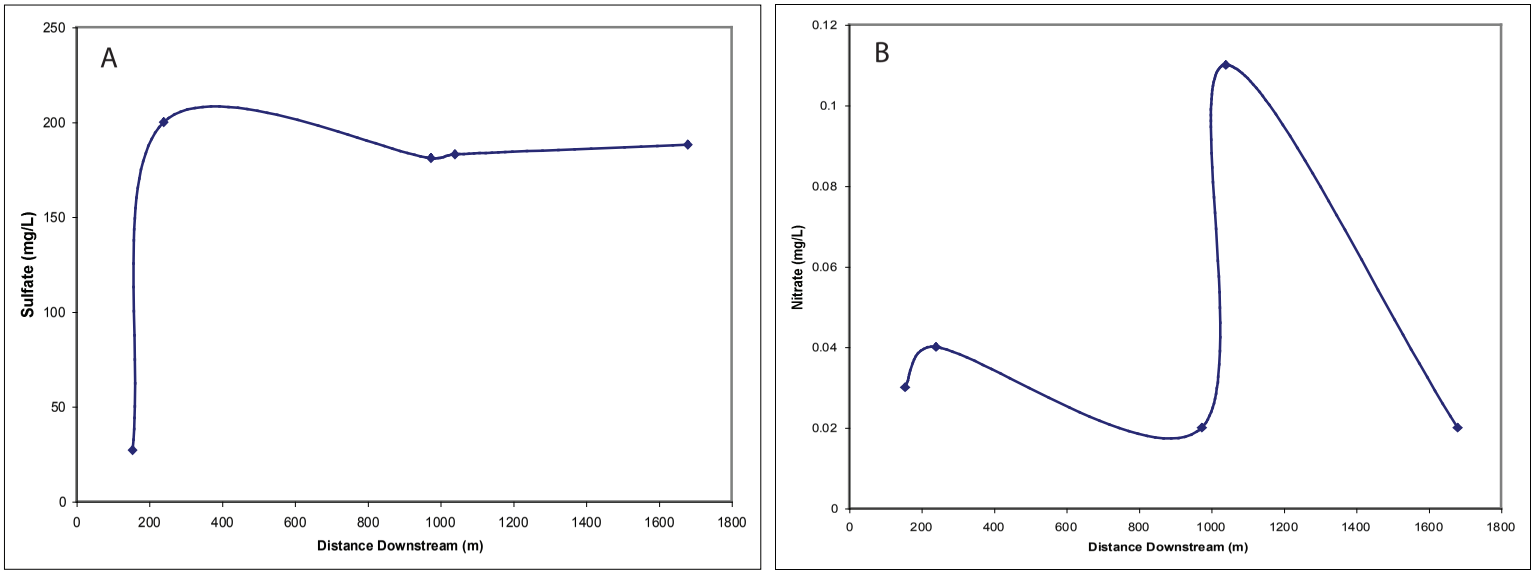

Figure 9. A)Sulfate concentrations behave similar to dissolved metals due to its ability to sorb onto precipitates. B) Nitrate concentrations increase at the inflow of each tributary then decrease downstream.

from solution; however, BOT, E-470, E-470 portal and LLBC-3 have positive saturation indices for different sets of minerals (Table 4). The Blow Out Tributary demonstrates the highest number of supersaturated minerals; however the saturation indices remain relatively small, indicating a lower tendency toward precipitation. The E-470 Tributary is supersaturated with respect to iron rich minerals, kaolinite and quartz.

Water from LLBC-3 is superstaturated with respect to goethite, hematite, kaolinite and quartz. Minerals with aluminum present in their chemical structure have the highest saturation indices after the confluence of Little Backbone Creek and the Blow Out Tributary then decrease downstream, while minerals with iron in the chemical structure have saturation indices that increase downstream. The exception is LLBC-9 which is impacted by water from Lake Shasta.

Precipitate samples from LLBC-3 and LLBC-4 display d-spacings that correspond primarily to gibbsite (4.37 Å and 2.39 Å d-spacing). Hematite (2.70 Å and 2.52 Å d-spacing) and goethite (4.18 Å, 2.45 Å and 2.69 Å d-spacing) are also present in small amounts. Precipitate samples from LLBC-6 and LLBC-7 have d-spacing corresponding to gibbsite and kaolinite (7.17 Å, 3.58 Å and 2.29 Å d-spacing) with minor amounts of goethite and hematite. Precipitate from LLBC-8 displays peaks corresponding to hematite and goethite. In addition to peaks associated with the identified minerals, all XRD scans of the precipitates display high background intensities, which suggest the presence of amorphous forms of these minerals.

Precipitate particles that tend to exhibit smooth surfaces with cleavage along the 001 axis and a tendency toward a hexagonal crystal structure have compositions rich in aluminum, silica, and oxygen with components of potassium and sulfur. In contrast,

TABLE 4. PRECIPITATE SATURATION INDICES

Pricipitating Mineral		LLBC-3	BOT	LLBC-4	LLBC-7	E-470 Trib.	LLBC-8	LLBC-9	E-470 Portal
Alunite	$KAl_3(SO_4)_2(OH)_6$		4.22	5.99	5.7		5.67	4.93	
Ca-Montmorillonite	$CaMg_6(Si_4O_{10})_3(OH)_6\text{-}nH_20$	3.68	0.39	3.24	2.61		2.56	1.85	
Gibbsite	$Al(OH)_3$	2.18	0.55	1.85	1.68		1.66	1.34	
Goethite	FeOOH		3.72	3.83	4.09	1.8	4.34	4.23	0.18
Hematite	Fe_2O_3		9.41	9.62	10.15	5.59	10.65	10.43	2.31
Muscovite	$KAl_3Si_3O_{10}(OH)_2$		2.29	6.07	5.43		5.39	4.24	
Kaolinite	$Al_2Si_2O_5(OH)_4$	5.59	2.9	5.34	4.87	1.82	4.84	4.23	
Quartz	SiO_2	0.22	0.5	0.42	0.35	0.41	0.36	0.38	0.8

particles rich in iron and oxygen tend to display either a granular or a cubic structure, while particles with a high percentage of silica have a rough surface without any definable shape or cleavage.

The main purpose of SEM data collection was to determine the possibility of copper and zinc sorption onto the precipitates. The data indicate that zinc is not present in the crystal structure of any of the precipitates; however, there evidence that copper and sulfate adsorb to aluminum hydroxides. Iron oxide precipitates display a very low incidence of copper and sulfate adsorption.

DISCUSSION

Characterization of Iron Oxides

Precipitation of iron oxides in Little Backbone Creek results from the oxidation of soluble, ferrous iron to insoluble, ferric iron in the following chemical reaction (Jonsson et al., 2005; Hem, 1989):

$$Fe^{2+} + 0.25O_2 + H^+ \leftrightarrow Fe^{3+} + 0.5H_2O.$$

Concentrations of dissolved iron observed in Little Backbone Creek are equivalent to the concentration of ferrous iron in solution, while total iron is equivalent to the concentration of ferrous and ferric iron in the sample (Hem, 1989). Results indicate that the concentration of total iron is relatively constant between LLBC-4 and LLBC-7; however, the ferrous iron concentrations increase by approximately 0.04 mg/L indicating the reduction of ferric iron. The relative lack of chemical activity between ferrous and ferric iron indicates that the iron in the system is near or slightly above equilibrium between LLBC-4 and LLBC-7 (Hem, 1989). Precipitate samples collected from the

stream channel at locations LLBC-5, LLBC-6, and LLBC-7 have only trace amounts of iron oxides. However, the presence of iron oxides in the precipitate increases slightly downstream as seen in the SEM data and the increase in the positive saturation.

In this study, observed variations in precipitation correspond to a slight decrease in pH downstream from LLBC-5. When sampling the water of Little Backbone Creek, the 5.1 Tributary (Figure 3) was initially ignored as the flow of the stream was negligible with respect to the flows at the Blow Out Tributary and the E-470 Tributary, yet inflow from this stream seems to alter the pH of Little Backbone Creek. This change in the geochemistry may be related to the increased precipitation of iron oxides, as goethite and hematite or ferrihydrate ($5Fe_2O_3 \cdot 9H_2O$) tend to form at a pH above 4.5 (Bigham et al., 1996).

Study observations indicate iron oxides become the dominant precipitate seen along Little Backbone Creek after the confluence of the E-470 Tributary. The E-470 Tributary has a significantly higher concentration of iron and lower concentrations of other metals relative to Little Backbone Creek. The rapid increase in iron concentrations results in changes in the water geochemistry, including an increase in oxidation-reduction potential and electrical conductivity.

As the oxidation rate of ferrous iron is highly dependent on pH, the slight change in the pH at LLBC-5 and the increase in total iron concentrations results in an increase in the precipitation of iron oxides (Figure 6) (Jonsson et al., 2005; Sidenko and Sherriff, 2005). The increase in iron oxide precipitation can be seen the sharp increase in the saturation indices of hematite and goethite in contrast to the decreasing saturation indices of other minerals in Little Backbone Creek (Parkhurst, 1999). In addition, results indicate

that precipitation of hematite and goethite corresponds to a decrease in the concentrations of both total and dissolved iron. The decrease in total iron corresponds to the precipitation of ferric iron as iron hydroxides, while the relatively smaller decrease in dissolved iron is related to equilibrium oxidation of ferrous iron (Jonsson et al., 2005; Hem, 1989).

Although the water associated with the precipitation of iron oxides have distinct geochemical characteristics, the identification of the specific minerals may be difficult (Murad and Rojik, 2003). Often, it is only possible to identify these minerals as iron oxides and hydroxides (Munk, 2002). This study uses a combination of SEM, XRD, and saturation indices the iron oxides precipitating along Little Backbone Creek can be fairly well defined. The PHREEQC geochemical model predicts supersaturation of goethite and hematite with respect to solution. The d-spacing peaks correspond to the predictions made by the geochemical model, yet the SEM data indicates a large percentage of sulfur as part of the iron oxides.

Jarosite tends to precipitate at a pH of less than 2.8, while schwertmannite dominates between a pH of 2.8, and goethite, ferrihydrate and hematite precipitate above a pH of 4.5 (Bigham et al., 1996; Jonsson et al., 2005). This regime agrees well with the data, indicating the precipitation of goethite and hematite along Little Backbone Creek, as the pH of the water ranges from 4.3 to 4.9. Ferrihydrate is frequently seen in precipitates forming in acidic mine drainage (Jonsson et al., 2005; Murad and Rojik, 2005). The lack of ferrihydrate in the precipitate samples may result because it is a hydrous form of hematite, and may not be accounted for in the geochemical model (Parkhurst, 1999).

Goethite precipitated in acid mine drainage environments is generally relatively well crystallized and can be identified by XRD even when present in small amounts (Murad and Rojik, 2005). Yet in this study, XRD scans from samples collected at LLBC-8, displayed high background intensities relative to peak intensity indicating the presence of amorphous iron precipitates, agreeing with the results of Rose and Elliott (2000).

Though both geochemical modeling and XRD data indicate that the main components of the precipitate from LLBC-7 to LLBC-9 are hematite and goethite, the SEM data indicate the presence of aluminum in the chemical composition of the iron hydroxides. Herbert (1997) report the presence of aluminum in the crystal structure occurs frequently as goethite is rarely pure in nature and the substitution of aluminum for iron occurs frequently during formation.

Characterization of Aluminum Hydroxides

The precipitation of aluminum hydroxides occurs when the decrease in pH associated with the neutralization of acid mine drainage forces dissolved aluminum out of solution (Stumm and Morgan, 1996; Munk et al., 2002; Ranville et al., 2004). The results show that the acidic water of the Blow Out Tributary is neutralized by mixing with Little Backbone Creek, resulting in significant precipitation of aluminum hydroxides between LLBC-4 and LLBC-7. The precipitation of aluminum hydroxides corresponds to the decrease in dissolved aluminum (Figure 6). Geochemical modeling results predict the precipitation of both gibbsite and kaolinite, which is confirmed by the presence of both minerals in the XRD results. The stability of gibbsite and kaolinite in Little Backbone

Creek agree with Nordstrom and Ball's (1986) conclusion that natural waters tend to be saturated with respect to aluminum hydroxides above a pH of 4.5.

PHREEQC also predicts a fairly high saturation index for alunite, an aluminum sulfate which, based on the results, is not present in the precipitate samples. Results by Nordstrom and Ball (1986) show that the cessation of alunite precipitation and the corresponding onset of gibbsite precipitation is related to the first hydrolysis constant for aluminum which occurs between pH values of 4.6 and 4.9. This disequilibrium in the natural system is not accounted for in the model, which may result in an inaccurate saturation index for alunite.

The results indicate that the presence of both gibbsite and kaolinite decreases rapidly with the mixing of water from the E-470 Tributary and Little Backbone Creek. The decrease in kaolinite and gibbsite precipitates is likely the result of the slight drop in pH associated with the inflow from the 5.1 Tributary, and the increase in iron concentrations associated with the inflow from the E-470 Tributary. The pH of Little Backbone Creek falls in the transition (pH 4.5 to 5.0) between the conservative and nonconservative behavior of aluminum as defined by Nordstrom and Ball (1986). This conclusion agrees with the results of the study, which indicates that it is likely that geochemical changes in water geochemistry result in dissolved aluminum transitioning from nonconservative to conservative behavior Between LLBC-7 and LLBC-8. The lack of aluminum hydroxide precipitates also agrees with this conclusion.

This study demonstrates that precipitation of gibbsite and kaolinite occurs in Little Backbone Creek; however, SEM analysis indicates that there are both sulfur and copper

in the chemical structure of the precipitates which are most likely associated with adsorption onto exposed mineral faces.

Characterization of Trace Precipitates

PHREEQC results indicate several trace minerals may precipitate along Little Backbone Creek in association with aluminum hydroxides and iron oxides. These minerals include muscovite, quartz, and calcium rich montmorillonite. Due to the small precipitate sample size and the lack of trace mineral identification with both XRD and SEM, it is difficult to determine the presence of these minerals in the precipitate. However, both Lee (2001) and Edraki et al. (2005) indicate that minor amounts of these and other minerals are a component of precipitates related to acid mine drainage suggest that the presence of these minerals in Little Backbone Creek is likely.

Copper and Sulfate Adsorption

SEM data show that aluminum precipitates observed along Little Backbone Creek display adsorption of trace metals and sulfates. This adsorption occurs frequently when acid mine drainage is neutralized by surface water (Munk et al., 2000, Munk et al., 2002; Ranville et al. 2004; Sidenko and Sherriff, 2005; Jonsson et al., 2006). However, the rate of trace metal sorption is low in Little Backbone Creek as the sorption of copper and zinc is limited at a low pH (Sidenko and Sherriff, 2005). While Little Backbone Creek has a pH of approximately 4.8, cations favor sorption from pH 5 to 6 (Jonsson et al., 2006). The tendency of trace metals to adsorb to precipitate surfaces decreases at a lower pH because the surface sites become less positive (Dzombak and Morel, 1990; Sidenko and

Sherriff, 2005; Jonsson et al., 2006). This agrees with SEM data which shows a relatively low (approximately one percent) sorption of copper on kaolinite and gibbsite. This result agrees with data collected by Ranville et al. (2004).

The presence of copper without the adsorption of other trace metals agrees with the conclusions of Sidenko and Sherriff (2005) which indicate that the affinity of trace metals in acid mine drainage to precipitate follows the order of copper > zinc > nickel. Yet, the water geochemistry results indicate that dissolved zinc concentrations decrease between LLBC-4 and LLBC-7, without associated adsorption onto aluminum hydroxides. It is possible that the water geochemistry is such that zinc precipitates out of solution; however, the pH is low enough that only trace metals with a higher affinity such as copper adsorb to aluminum precipitate surface sites. The affinity of zinc cations for surface attenuation is low enough that there is little sorption of zinc on precipitate surface sites.

The lack of copper sorption to the iron oxides is surprising as there is only minor change in the pH of Little Backbone Creek though similar results are presented by Tonkin et al. (2002). However, McKnight et al. (1992) report that there is a decrease in trace metal sorption on iron oxides as the organic content of the surrounding water decreases indicating that trace metal content on iron oxides may be caused by complexion of the trace metals to organic material adsorbed to the iron oxides instead of direct sorption onto iron oxides. The streambed of Little Backbone Creek is either gravel or bedrock as are the streambed of the tributaries, thus it is likely that there are only trace amount of organic materials. This lack of organic material would limit organic complexion sites resulting in little adsorption of copper or zinc to the surface of the iron

oxides as demonstrated by McKnight et al. (1992). In addition, the lack of trace metal adsorption onto iron oxides would also account for the conservative behavior of dissolved copper and zinc after the inflow of the E-470 Tributary.

Negatively charged sulfate molecules act in a similar manner to copper and adsorb to the surface of aluminum hydroxides at a relatively low pH (Dzombak and Morel, 1990; Rothenhofer et al., 1999; Ranville et al., 2004; Munk et al., 2002). The results of this study confirm this, as the adsorption of sulfate follows the pattern of trace metal sorption in Little Backbone Creek. The presence of sulfur on aluminum hydroxides in the SEM data agrees with the results of Rothenhofer et al. (1999) which indicate that at pH values around 4.8 precipitates of aluminum hydroxides tend to adsorb sulfate on surface complexion sites. However, sulfate adsorption does not seem to occur on iron oxide precipitates.

The concentrations of trace metals in acidic mine drainage is often above the limits imposed by the Clean Water Act as implemented by the State of California. High concentrations of dissolved metals has a destructive impact on aquatic life. Thus, removing dissolved trace metals to enhance aquatic habitat may be possible due to the tendency of trace metals to adsorb to the surface of aluminum and iron hydroxides. Munk et al. (2002) and Ranville et al. (2004) both demonstrate that at specific pH ranges the solubility of trace metals can be reduced causing precipitation and sorption to aluminum and iron oxides. Data from a neutralization experiment by Munk et al. (2002) indicate that approximately 90% of dissolve copper is adsorbed at a pH of 6.0, while maximum zinc sorption occurs near a pH of 7. In fact, actively treating acid mine drainage with calcium carbonate, sodium hydroxide, sodium bicarbonate or anhydrous ammonia in

order to increase the pH of the water and decrease trace metal solubility is often a remediation option at abandoned mine sites. However, the unintentional lowering of pH may cause desorption of trace metals from the surface of aluminum and iron oxides limiting any benefits of natural trace metal sorption (Munk and Faure, 2004).

Further Research

Though this study yielded interesting results that correspond with current research; however, a more quantitative analysis of precipitate chemistry and a better understanding of significant geochemical changes could result from the controlled titration of water from Little Backbone Creek. This would yield more homogenous precipitates for analysis and more precise picture of geochemical changes could be observed. Furthermore, there is a large body of work regarding the precipitation of aluminum and iron oxides from acidic mine water; however, identification of the resulting precipitates and the geochemical changes in the water are still difficult due to the nature of the precipitate formation. Thus, the field would benefit from further rigorous geochemical analysis and better defined parameters for precipitates.

CONCLUSIONS

The Blow Out Tributary and the E-470 Tributary contain concentrated amounts of acid mine drainage enriched with aluminum, iron and trace metals. The confluence of these tributaries and Little Backbone Creek results in the neutralization of acid mine waters and the corresponding precipitation of aluminum hydroxides and iron oxides.

Gibbsite and kaolinite dominate the precipitates from LLBC-4 to LLBC-7 while goethite and hematite are the main constituents in the precipitate resulting from the mixing of the E-470 tributary and Little Backbone Creek. The change in precipitate content is the result of a slight change in the pH of Little Backbone Creek and an increase in iron concentrations from the E-470 Tributary.

Adsorption of copper and sulfate is seen on surface sites of aluminum oxides throughout the field site. However, there is no adsorption of trace metals or sulfate on iron oxides most likely due to the absence organic material to aid complexion.

Little Backbone Creek is similar to streams affected by acid mine drainage throughout the world. Elevated concentrations of aluminum, iron, and trace metals result in the precipitation of a variety aluminum and iron minerals with chemical characteristics that are determined primarily by the pH of the surrounding water.

ACKNOWLEDGEMENTS

First and foremost, I would like to thank Mining Remedial Recovery Company for providing site access, background information, historical data and financial support for laboratory analyses. I would also like to thank VESTRA Resources for additional analytical support and technical support. In addition, I would like to acknowledge all the individuals at VESTRA Resources for their humor and encouragement through the entire process.

I would like to extend special recognition to Bruce Hauser and Jason Hauser of Mining Remedial Recovery Company and Reed Andrews for providing transport across

Lake Shasta, for assistance with field work and heavy lifting, and for feigning interest in both directions.

I would like to acknowledge the assistance of my advisor, Bereket Haileab and finally, the support of the geology majors of 2007.

REFERENCES

Bigham, J. M., Schwertmann, U., Traina, S. J., Winland, R. L., and Wolf, M., 1996, Schwertmannite and the chemical modeling of iron in acid sulfate waters: Geochimica Et Cosmochimica Acta, v. 60, no. 12, p. 2111-2121.

Bowell, R. J., and Bruce, I., 1995, Geochemistry of iron ochres and mine waters from Levant Mine, Cornwall: Applied Geochemistry, v. 10, no. 2, p. 237-250.

California Department of Water Resources, 2006, California Data Exchange Center: Shasta Dam Station, p. Department of Water Resources Operational Hydrologic Data.

DaSilva, E. F., Patinha, C., Reis, P., Fonseca, E. C., Matos, J. X., Barrosinho, J., and Oliveira, J. M. S., 2006, Interaction of acid mine drainage with waters and sediments at the Corona Stream, Lousal Mine (Iberian Pyrite Belt, Southern Portugal): Environmental Geology, v. 50, no. 7, p. 1001-1013.

Dzombak, D. A., and Morel, F., 1990, Surface complexion modeling: Hydrous ferric oxide: New York, Wiley.

Edraki, M., Golding, S. D., Baublys, K. A., and Lawrence, M. G., 2005, Hydrochemistry, mineralogy and sulfur isotope geochemistry of acid mine drainage at the Mt. Morgan mine environment, Queensland, Australia: Applied Geochemistry, v. 20, no. 4, p. 789-805.

Espana, J. S., Pamo, E. L., Pastor, E. S., Andres, J. R., and Rubi, J. A. M., 2006, The impact of acid mine drainage on the water quality of the Odiel River (Huelva, Spain): Evolution of precipitate mineralogy and aqueous geochemistry along the Concepcion-Tintillo segment: Water Air and Soil Pollution, v. 173, no. 1-4, p. 121-149.

Gammons, C. H., Nimick, D. A., Parker, S. R., Cleasby, T. E., and McCleskey, R. B., 2005, Diel behavior of iron and other heavy metals in a mountain stream with acidic to neutral pH: Fisher Creek, Montana, USA: Geochimica Et Cosmochimica Acta, v. 69, no. 10, p. 2505-2516.

Hem, J. D., 1989, Study and interpretation of the chemical characteristics of natural water, United States Geological Survey Water-Supply Paper 2254: Washington, D.C., United States Government Printing office, 263 p.

Herbert, R. B., 1997, Properties of goethite and jarosite precipitated from acidic groundwater, Dalarna, Sweden: Clays and Clay Minerals, v. 45, no. 2, p. 261-273.

Jonsson, J., Jonsson, J., and Lovgren, L., 2006, Precipitation of secondary Fe(III) minerals from acid mine drainage: Applied Geochemistry, v. 21, no. 3, p. 437-445.

Kawano, M., and Tomita, K., 2001, Geochemical modeling of bacterially induced mineralization of schwertmannite and jarosite in sulfuric acid spring water: American Mineralogist, v. 86, no. 10, p. 1156-1165.

Kinkel, A. R., and Hall, W. E., 1952, Geology of the Mammoth Mine, Shasta County, California.

Kinkel, A. R., Hall, W. E., and Alpers, J. P., 1956, Geology and Base-Metal Deposits of West Shasta Copper- Zinc District, Shasta County, California Geological Survey Professional Paper 285, *in* Interior, U. S. D. o. t., and State of California, D. o. N. R., Division of Mines, eds., United States Government Printing Office, p. 1-158.

Kristofers, K. V., 1973, The copper mining era in Shasta County, California, 1896-1919: An environmental impact study [Chico State University Master's Thesis thesis]: Chico State University, 126 p.

Lee, C. H., Lee, H. K., and Lee, J. C., 2001, Hydrogeochemistry of mine, surface and groundwaters from the Sanggok mine creek in the upper Chungju Lake, Republic of Korea: Environmental Geology, v. 40, no. 4-5, p. 482-494.

McKnight, D., and Bencala, K. E., 1988, Diel Variations in iron chemistry in an acidic stream in the Colorado Rocky-Mountains, USA: Arctic and Alpine Research, v. 20, no. 4, p. 492-500.

McKnight, D. M., Wershaw, R. L., Bencala, K. E., Zellweger, G. W., and Feder, G. L., 1992, Humic substances and trace-metals associated with Fe and Al oxides deposited in an acidic mountain stream: Science of the Total Environment, v. 118, p. 485-498.

Munk L., F. G., Pride D.E., Bigham J.M., 2002, Sorption of trace metals to an aluminum precipitate in a stream receiving acid rock-drainage; Snake River, Summit County, Colorado: Applied Geochemistry, v. 17, no. 4, p. 421-430.

Munk, L. A., and Faure, G., 2004, Effects of pH fluctuations on potentially toxic metals in the water and sediment of the Dillon Reservoir, Summit County, Colorado: Applied Geochemistry, v. 19, no. 7, p. 1065-1074.

Murad, E., and Rojik, P., 2003, Iron-rich precipitates in a mine drainage environment: Influence of pH on mineralogy: American Mineralogist, v. 88, no. 11-12, p. 1915-1918.

Murad, E., and Rojik, P., 2005, Iron mineralogy of mine-drainage precipitates as environmental indicators: review of current concepts and a case study from the Sokolov Basin, Czech Republic: Clay Minerals, v. 40, no. 4, p. 427-440.

Nordstrom, D. K., and Ball, J. W., 1986, The geochemical behavior of aluminum in acidified surface waters: Science, v. 232, no. 4746, p. 54-56.

Parker, S. R., Gammons, C.H. Nimick, D.A., 2004, Importance on the diel cycling of metals in Fisher Creek, Montana.

Parkhurst, D. L., and Appelo, C. A. J., 1999, User's Guide to PHREEQC (Version 2) - A computer program for speciation, batch-reaxtion, one-dimensional transport, and inverse geochemical calculations U. S. Department of the Interior.

Potter, R. W., 1976, The weathering of sulfide ores in Shasta County, California, and its relationship to pollution associated with acid mine drainage, *in* Interior, U. S. D. o. t., ed., United States Geological Survey.

Ranville, M., Rough, D., and Flegal, A. R., 2004, Metal attenuation at the abandoned Spenceville copper mine: Applied Geochemistry, v. 19, no. 5, p. 803-815.

Rose, S., and Elliott, W. C., 2000, The effects of pH regulation upon the release of sulfate from ferric precipitates formed in acid mine drainage: Applied Geochemistry, v. 15, no. 1, p. 27-34.

Rothenhofer, P., Sahin, H., and Peiffer, S., 1999, Attenuation of heavy metals and sulfate by aluminium precipitates in acid mine drainage?: Acta Hydrochimica Et Hydrobiologica, v. 28, no. 3, p. 136-144.

Sidenko, N. V., and Sherriff, B. L., 2005, The attenuation of Ni, Zn and Cu, by secondary Fe phases of different crystallinity from surface and ground water of two sulfide mine tailings in Manitoba, Canada: Applied Geochemistry, v. 20, no. 6, p. 1180-1194.

Stumm, W., and Morgan, J. J., 1996, Aquatic Chemistry: New York, Wiley.

Tonkin, J. W., Balistrieri, L. S., and Murray, J. W., 2002, Modeling metal removal onto natural particles formed during mixing of acid rock drainage with ambient surface water: Environmental Science & Technology, v. 36, no. 3, p. 484-492.

VESTRA Resources, and Mining Remedial Recovery Company, 2005, Use attainability analysis: West Squaw Creek Watershed, Shasta County, California: VESTRA Resources.

Wentz, D. A., 1974, Stream quality in relation to acid mine drainage in Colorado, *in* Water Resource Problems Related to Mining, Minneapolis, Minnesota, p. 158-173.

Appendix 1
Distribution of species in each modeling run has been removed for brevity.

```
DATABASE C:\Program Files\USGS\Phreeqc Interactive 2.13.2\phreeqc.dat
        SOLUTION 1 BOT
          temp      17.7
          pH        4.4
          pe        9.04
          redox     pe
          units     mg/kgw
          density   1
          Alkalinity 0
          Al        17200 ug/kgw
          Ca        45
          Cu        3140 ug/kgw
          Fe        88 ug/kgw
          Mg        13
          K         0.7
          Si        15.5
          Na        5
          Zn        6320 ug/kgw
          Cl        0
          N         0.03
          S(6)      332
          water     1 # kg
-------------------------------------------
Beginning of initial solution calculations.
-------------------------------------------

Initial solution 1.       BOT

-----------------------------Solution composition------------------------------

        Elements           Molality       Moles

        Al              6.375e-004  6.375e-004
        Ca              1.123e-003  1.123e-003
        Cu              4.941e-005  4.941e-005
        Fe              1.576e-006  1.576e-006
        K               1.790e-005  1.790e-005
        Mg              5.347e-004  5.347e-004
        N               2.142e-006  2.142e-006
        Na              2.175e-004  2.175e-004
        S(6)            3.456e-003  3.456e-003
        Si              2.580e-004  2.580e-004
        Zn              9.668e-005  9.668e-005
```

----------Description of solution----------

pH = 4.400
pe = 9.040
Activity of water = 1.000
Ionic strength = 9.347e-003
Mass of water (kg) = 1.000e+000
Total alkalinity (eq/kg) = -3.006e-005
Total carbon (mol/kg) = 0.000e+000
Total CO2 (mol/kg) = 0.000e+000
Temperature (deg C) = 17.700
Electrical balance (eq) = -1.124e-003
Percent error, 100*(Cat-|An|)/(Cat+|An|) = -11.87
Iterations = 9
Total H = 1.110135e+002
Total O = 5.552109e+001

----------Saturation indices----------

Phase	SI	log IAP	log KT	
Al(OH)3(a)	-2.21	9.08	11.29	Al(OH)3
Albite	-5.96	-24.44	-18.48	NaAlSi3O8
Alunite	4.22	3.75	-0.48	KAl3(SO4)2(OH)6
Anhydrite	-1.61	-5.95	-4.34	CaSO4
Anorthite	-10.38	-30.31	-19.93	CaAl2Si2O8
Ca-Montmorillonite	0.39	-45.71	-46.10	Ca0.165Al2.33Si3.67O10(OH)2
Chalcedony	0.05	-3.59	-3.64	SiO2
Chlorite(14A)	-37.41	33.76	71.17	Mg5Al2Si3O10(OH)8
Chrysotile	-24.49	8.64	33.13	Mg3Si2O5(OH)4
Fe(OH)3(a)	-1.91	2.98	4.89	Fe(OH)3
Gibbsite	0.55	9.08	8.53	Al(OH)3
Goethite	3.72	2.98	-0.73	FeOOH
Gypsum	-1.37	-5.95	-4.58	CaSO4:2H2O
H2(g)	-26.88	-30.00	-3.12	H2
H2O(g)	-1.70	-0.00	1.70	H2O
Hematite	9.41	5.97	-3.44	Fe2O3
Illite	-3.24	-44.52	-41.27	K0.6Mg0.25Al2.3Si3.5O10(OH)2
Jarosite-K	-5.90	-14.54	-8.63	KFe3(SO4)2(OH)6
K-feldspar	-4.38	-25.52	-21.14	KAlSi3O8
K-mica	2.29	16.08	13.80	KAl3Si3O10(OH)2
Kaolinite	2.90	10.98	8.08	Al2Si2O5(OH)4
Melanterite	-6.50	-8.81	-2.30	FeSO4:7H2O
N2(g)	-2.73	-5.97	-3.24	N2

```
        NH3(g)         -38.59  -36.67    1.92  NH3
        O2(g)          -31.96  -34.80   -2.84  O2
        Quartz           0.50   -3.59   -4.09  SiO2
        Sepiolite      -16.18   -0.22   15.96  Mg2Si3O7.5OH:3H2O
        Sepiolite(d)   -18.88   -0.22   18.66  Mg2Si3O7.5OH:3H2O
        SiO2(a)         -0.81   -3.59   -2.77  SiO2
        Talc           -20.79    1.47   22.25  Mg3Si4O10(OH)2
        Willemite      -10.51    5.44   15.94  Zn2SiO4
        Zn(OH)2(e)      -6.99    4.51   11.50  Zn(OH)2

------------------
End of simulation.
------------------
------------------------------------
Reading input data for simulation 2.
------------------------------------
-----------
End of run.
-----------

DATABASE C:\Program Files\USGS\Phreeqc Interactive 2.13.2\phreeqc.dat
        SOLUTION 1 E-470 Portal
           temp      14
           pH        2.1
           pe        9.22
           redox     pe
           units     mg/kgw
           density   1
           Al        45400 ug/kgw
           Ca        109
           Cu        27500 ug/kgw
           Fe        383000 ug/kgw
           Mg        38
           K         0.3
           Si        32.1
           Na        7
           Zn        55300 ug/kgw
           Cl        0
           N         0.06
           S(6)      2310
           Alkalinity 0
           water     1 # kg
-------------------------------------------
Beginning of initial solution calculations.
-------------------------------------------
```

Initial solution 1. E-470 Portal

----------Solution composition----------

Elements	Molality	Moles
Al	1.683e-003	1.683e-003
Ca	2.720e-003	2.720e-003
Cu	4.328e-004	4.328e-004
Fe	6.858e-003	6.858e-003
K	7.672e-006	7.672e-006
Mg	1.563e-003	1.563e-003
N	4.284e-006	4.284e-006
Na	3.045e-004	3.045e-004
S(6)	2.405e-002	2.405e-002
Si	5.342e-004	5.342e-004
Zn	8.460e-004	8.460e-004

----------Description of solution----------

pH = 2.100
pe = 9.220
Activity of water = 0.999
Ionic strength = 5.269e-002
Mass of water (kg) = 1.000e+000
Total alkalinity (eq/kg) = -1.417e-002
Total carbon (mol/kg) = 0.000e+000
Total CO2 (mol/kg) = 0.000e+000
Temperature (deg C) = 14.000
Electrical balance (eq) = -3.740e-003
Percent error, 100*(Cat-|An|)/(Cat+|An|) = -6.20
Iterations = 12
Total H = 1.110287e+002
Total O = 5.560454e+001

----------Saturation indices----------

Phase	SI	log IAP	log KT	
Al(OH)3(a)	-9.48	2.07	11.54	Al(OH)3
Albite	-14.37	-33.10	-18.73	NaAlSi3O8
Alunite	-9.74	-9.73	0.01	KAl3(SO4)2(OH)6
Anhydrite	-0.95	-5.29	-4.33	CaSO4
Anorthite	-28.96	-48.99	-20.04	CaAl2Si2O8
Ca-Montmorillonite	-15.91	-62.57	-46.67	Ca0.165Al2.33Si3.67O10(OH)2
Chalcedony	0.42	-3.27	-3.68	SiO2

```
        Chlorite(14A)   -73.82   -1.18   72.63  Mg5Al2Si3O10(OH)8
        Chrysotile      -37.46   -3.84   33.61  Mg3Si2O5(OH)4
        Fe(OH)3(a)       -5.31   -0.42    4.89  Fe(OH)3
        Gibbsite         -6.68    2.07    8.75  Al(OH)3
        Goethite          0.18   -0.42   -0.59  FeOOH
        Gypsum           -0.70   -5.29   -4.59  CaSO4:2H2O
        H2(g)          -22.64  -25.74   -3.10  H2
        H2O(g)           -1.81   -0.00    1.81  H2O
        Hematite          2.31   -0.83   -3.14  Fe2O3
        Illite         -21.40  -63.20  -41.80  K0.6Mg0.25Al2.3Si3.5O10(OH)2
        Jarosite-K       -8.85  -17.18   -8.33  KFe3(SO4)2(OH)6
        K-feldspar      -13.27  -34.71  -21.44  KAlSi3O8
        K-mica          -21.09   -6.72   14.37  KAl3Si3O10(OH)2
        Kaolinite       -10.83   -2.40    8.43  Al2Si2O5(OH)4
        Melanterite      -2.50   -4.85   -2.35  FeSO4:7H2O
        N2(g)            -2.44   -5.66   -3.22  N2
        NH3(g)          -31.98  -29.98    2.00  NH3
        O2(g)           -41.78  -44.59   -2.80  O2
        Quartz           0.88   -3.27   -4.15  SiO2
        Sepiolite       -24.07   -8.01   16.06  Mg2Si3O7.5OH:3H2O
        Sepiolite(d)    -26.67   -8.01   18.66  Mg2Si3O7.5OH:3H2O
        SiO2(a)          -0.46   -3.27   -2.81  SiO2
        Talc            -33.08  -10.38   22.70  Mg3Si4O10(OH)2
        Willemite       -18.40   -2.14   16.27  Zn2SiO4
        Zn(OH)2(e)      -10.93    0.57   11.50  Zn(OH)2

------------------
End of simulation.
------------------
------------------------------------
Reading input data for simulation 2.
------------------------------------
-----------
End of run.
-----------


DATABASE C:\Program Files\USGS\Phreeqc Interactive 2.13.2\phreeqc.dat
        SOLUTION 1 E-470 Trib
          temp      21.8
          pH        4.1
          pe        7.36
          redox     pe
          units     mg/kgw
          density   1
          Alkalinity 0
```

Cl	0
N	0
S(6)	231
Al	7190 ug/kgw
Ca	33
Cu	1340 ug/kgw
Fe	203 ug/kgw
Mg	13
K	0
Si	14.5
Na	5
Zn	3830 ug/kgw
water	1 # kg

Beginning of initial solution calculations.

Initial solution 1. E-470 Trib

----------Solution composition----------

Elements	Molality	Moles
Al	2.665e-004	2.665e-004
Ca	8.234e-004	8.234e-004
Cu	2.109e-005	2.109e-005
Fe	3.635e-006	3.635e-006
Mg	5.347e-004	5.347e-004
Na	2.175e-004	2.175e-004
S(6)	2.405e-003	2.405e-003
Si	2.413e-004	2.413e-004
Zn	5.859e-005	5.859e-005

----------Description of solution----------

pH = 4.100
pe = 7.360
Activity of water = 1.000
Ionic strength = 6.925e-003
Mass of water (kg) = 1.000e+000
Total alkalinity (eq/kg) = -9.075e-005
Total carbon (mol/kg) = 0.000e+000
Total CO2 (mol/kg) = 0.000e+000
Temperature (deg C) = 21.800
Electrical balance (eq) = -8.189e-004
Percent error, 100*(Cat-|An|)/(Cat+|An|) = -11.60

```
                    Iterations =   5
                      Total H  = 1.110135e+002
                      Total O  = 5.551681e+001

-----------------------------Saturation indices-------------------------------

        Phase               SI log IAP  log KT

        Al(OH)3(a)      -3.13    7.88   11.01  Al(OH)3
        Albite          -7.36  -25.57  -18.21  NaAlSi3O8
        Anhydrite       -1.82   -6.16   -4.35  CaSO4
        Anorthite      -12.77  -32.58  -19.81  CaAl2Si2O8
        Ca-Montmorillonite  -2.20  -47.69  -45.49  Ca0.165Al2.33Si3.67O10(OH)2
        Chalcedony      -0.03   -3.62   -3.59  SiO2
        Chlorite(14A)   -41.18   28.41   69.58  Mg5Al2Si3O10(OH)8
        Chrysotile      -25.74    6.86   32.60  Mg3Si2O5(OH)4
        Fe(OH)3(a)      -3.98    0.91    4.89  Fe(OH)3
        Gibbsite        -0.41    7.88    8.29  Al(OH)3
        Goethite         1.80    0.91   -0.88  FeOOH
        Gypsum          -1.58   -6.16   -4.58  CaSO4:2H2O
        H2(g)          -22.92  -26.06   -3.14  H2
        H2O(g)          -1.59   -0.00    1.59  H2O
        Hematite         5.59    1.82   -3.76  Fe2O3
        Kaolinite        0.82    8.53    7.72  Al2Si2O5(OH)4
        Melanterite     -6.26   -8.51   -2.25  FeSO4:7H2O
        O2(g)          -38.44  -41.31   -2.87  O2
        Quartz           0.41   -3.62   -4.03  SiO2
        Sepiolite       -17.30   -1.45   15.85  Mg2Si3O7.5OH:3H2O
        Sepiolite(d)    -20.11   -1.45   18.66  Mg2Si3O7.5OH:3H2O
        SiO2(a)         -0.88   -3.62   -2.74  SiO2
        Talc           -22.14   -0.37   21.77  Mg3Si4O10(OH)2
        Willemite       -11.75    3.84   15.60  Zn2SiO4
        Zn(OH)2(e)      -7.77    3.73   11.50  Zn(OH)2
------------------
End of simulation.
------------------
------------------------------------
Reading input data for simulation 2.
------------------------------------
-----------
End of run.
-----------


DATABASE C:\Program Files\USGS\Phreeqc Interactive 2.13.2\phreeqc.dat
        SOLUTION 1 LLBC-3
```

```
        temp      18.5
        pH        6.4
        pe        6.75
        redox     pe
        units     mg/kgw
        density   1
        Alkalinity 2
        Al        33 ug/kgw
        Ca        5
        Cu        58 ug/kgw
        Fe        0 ug/kgw
        Mg        2
        K         0
        Si        8.31
        Na        3
        Zn        247 ug/kgw
        Cl        0.17
        S(6)      27.1
        N         0.03
        water     1 # kg
-------------------------------------------
Beginning of initial solution calculations.
-------------------------------------------

Initial solution 1.       LLBC-3

-----------------------------Solution composition------------------------------

        Elements          Molality       Moles

        Al              1.223e-006  1.223e-006
        Alkalinity       3.996e-005  3.996e-005
        Ca              1.248e-004  1.248e-004
        Cl              4.795e-006  4.795e-006
        Cu              9.127e-007  9.127e-007
        Mg              8.226e-005  8.226e-005
        N               2.142e-006  2.142e-006
        Na              1.305e-004  1.305e-004
        S(6)            2.821e-004  2.821e-004
        Si              1.383e-004  1.383e-004
        Zn              3.778e-006  3.778e-006

----------------------------Description of solution----------------------------

                              pH  =   6.400
                              pe  =   6.750
```

Activity of water = 1.000
Ionic strength = 1.042e-003
Mass of water (kg) = 1.000e+000
Total carbon (mol/kg) = 7.116e-005
Total CO2 (mol/kg) = 7.116e-005
Temperature (deg C) = 18.500
Electrical balance (eq) = -5.139e-005
Percent error, 100*(Cat-|An|)/(Cat+|An|) = -4.56
Iterations = 9
Total H = 1.110130e+002
Total O = 5.550808e+001

----------Saturation indices----------

Phase	SI	log IAP	log KT	
Al(OH)3(a)	-0.57	10.66	11.23	Al(OH)3
Albite	-3.35	-21.78	-18.43	NaAlSi3O8
Anhydrite	-3.27	-7.61	-4.34	CaSO4
Anorthite	-4.40	-24.30	-19.90	CaAl2Si2O8
Aragonite	-4.13	-12.43	-8.30	CaCO3
Ca-Montmorillonite	3.68	-42.30	-45.98	Ca0.165Al2.33Si3.67O10(OH)2
Calcite	-3.98	-12.43	-8.45	CaCO3
Chalcedony	-0.23	-3.86	-3.63	SiO2
Chlorite(14A)	-17.93	52.92	70.85	Mg5Al2Si3O10(OH)8
Chrysotile	-14.83	18.19	33.02	Mg3Si2O5(OH)4
CO2(g)	-3.07	-4.46	-1.39	CO2
Dolomite	-8.10	-25.03	-16.94	CaMg(CO3)2
Gibbsite	2.18	10.66	8.48	Al(OH)3
Gypsum	-3.02	-7.61	-4.58	CaSO4:2H2O
H2(g)	-26.30	-29.42	-3.12	H2
H2O(g)	-1.68	-0.00	1.68	H2O
Halite	-10.80	-9.24	1.57	NaCl
Kaolinite	5.59	13.60	8.01	Al2Si2O5(OH)4
N2(g)	-2.73	-5.97	-3.24	N2
NH3(g)	-37.74	-35.84	1.90	NH3
O2(g)	-32.84	-35.68	-2.84	O2
Quartz	0.22	-3.86	-4.08	SiO2
Sepiolite	-10.24	5.70	15.93	Mg2Si3O7.5OH:3H2O
Sepiolite(d)	-12.96	5.70	18.66	Mg2Si3O7.5OH:3H2O
SiO2(a)	-1.09	-3.86	-2.77	SiO2
Smithsonite	-4.02	-13.95	-9.93	ZnCO3
Talc	-11.68	10.47	22.16	Mg3Si4O10(OH)2
Willemite	-5.15	10.73	15.88	Zn2SiO4
Zn(OH)2(e)	-4.21	7.29	11.50	Zn(OH)2

```
------------------
End of simulation.
------------------
------------------------------------
Reading input data for simulation 2.
------------------------------------
-----------
End of run.
-----------


DATABASE C:\Program Files\USGS\Phreeqc Interactive 2.13.2\phreeqc.dat
        SOLUTION 1 LLBC-4
           temp      16.7
           pH        4.9
           pe        8.13
           redox     pe
           units     mg/kgw
           density   1
           Alkalinity 0
           S(6)      200
           N         0.04
           Cl        0.93
           Al        9820 ug/kgw
           Ca        26
           Cu        1770 ug/kgw
           Fe        30 ug/kgw
           Mg        8
           K         0.3
           Si        12.5
           Na        4
           Zn        3520 ug/kgw
           water     1 # kg
-------------------------------------------
Beginning of initial solution calculations.
-------------------------------------------

Initial solution 1.       LLBC-4

-----------------------------Solution composition------------------------------

        Elements          Molality       Moles

        Al              3.640e-004  3.640e-004
        Ca              6.487e-004  6.487e-004
```

Cl	2.623e-005	2.623e-005
Cu	2.785e-005	2.785e-005
Fe	5.372e-007	5.372e-007
K	7.672e-006	7.672e-006
Mg	3.291e-004	3.291e-004
N	2.856e-006	2.856e-006
Na	1.740e-004	1.740e-004
S(6)	2.082e-003	2.082e-003
Si	2.080e-004	2.080e-004
Zn	5.385e-005	5.385e-005

----------Description of solution----------

pH = 4.900
pe = 8.130
Activity of water = 1.000
Ionic strength = 5.985e-003
Mass of water (kg) = 1.000e+000
Total alkalinity (eq/kg) = 3.546e-005
Total carbon (mol/kg) = 0.000e+000
Total CO2 (mol/kg) = 0.000e+000
Temperature (deg C) = 16.700
Electrical balance (eq) = -8.321e-004
Percent error, 100*(Cat-|An|)/(Cat+|An|) = -13.75
Iterations = 10
Total H = 1.110133e+002
Total O = 5.551543e+001

----------Saturation indices----------

Phase	SI	log IAP	log KT	
Al(OH)3(a)	-0.92	10.44	11.36	Al(OH)3
Albite	-4.51	-23.06	-18.55	NaAlSi3O8
Alunite	5.99	5.65	-0.35	KAl3(SO4)2(OH)6
Anhydrite	-1.96	-6.30	-4.34	CaSO4
Anorthite	-7.23	-27.19	-19.96	CaAl2Si2O8
Ca-Montmorillonite	3.24	-43.02	-46.25	Ca0.165Al2.33Si3.67O10(OH)2
Chalcedony	-0.03	-3.68	-3.65	SiO2
Chlorite(14A)	-31.16	40.40	71.56	Mg5Al2Si3O10(OH)8
Chrysotile	-22.28	10.98	33.26	Mg3Si2O5(OH)4
Fe(OH)3(a)	-1.76	3.13	4.89	Fe(OH)3
Gibbsite	1.85	10.44	8.59	Al(OH)3
Goethite	3.83	3.13	-0.70	FeOOH
Gypsum	-1.72	-6.30	-4.58	CaSO4:2H2O
H2(g)	-26.06	-29.17	-3.11	H2

```
        H2O(g)          -1.73   -0.00    1.73  H2O
        Halite          -9.98   -8.41    1.56  NaCl
        Hematite         9.62    6.26   -3.36  Fe2O3
        Illite          -0.26  -41.68  -41.41  K0.6Mg0.25Al2.3Si3.5O10(OH)2
        Jarosite-K      -7.72  -16.28   -8.55  KFe3(SO4)2(OH)6
        K-feldspar      -3.19  -24.41  -21.22  KAlSi3O8
        K-mica           6.07   20.02   13.95  KAl3Si3O10(OH)2
        Kaolinite        5.34   13.51    8.18  Al2Si2O5(OH)4
        Melanterite     -7.07   -9.38   -2.32  FeSO4:7H2O
        N2(g)           -2.61   -5.84   -3.23  N2
        NH3(g)          -37.27  -35.33    1.94  NH3
        O2(g)           -33.96  -36.79   -2.83  O2
        Quartz           0.42   -3.68   -4.11  SiO2
        Sepiolite       -14.80    1.18   15.98  Mg2Si3O7.5OH:3H2O
        Sepiolite(d)    -17.48    1.18   18.66  Mg2Si3O7.5OH:3H2O
        SiO2(a)         -0.90   -3.68   -2.78  SiO2
        Talc            -18.76    3.62   22.37  Mg3Si4O10(OH)2
        Willemite       -9.08    6.95   16.03  Zn2SiO4
        Zn(OH)2(e)      -6.19    5.31   11.50  Zn(OH)2

------------------
End of simulation.
------------------
------------------------------------
Reading input data for simulation 2.
------------------------------------
-----------
End of run.
-----------


DATABASE C:\Program Files\USGS\Phreeqc Interactive 2.13.2\phreeqc.dat
        SOLUTION 1 LLBC-7
          temp      19.5
          pH        4.8
          pe        8.26
          redox     pe
          units     mg/kgw
          density   1
          Cl        0
          N         0.02
          S(6)      181
          Alkalinity 0
          Al        8680 ug/kgw
          Ca        25
          Cu        1580 ug/kgw
```

```
        Fe      54 ug/kgw
        Mg       8
        K       0.4
        Si      11.7
        Na       4
        Zn      3220 ug/kgw
        water   1 # kg
-----------------------------------------
Beginning of initial solution calculations.
-----------------------------------------

Initial solution 1.       LLBC-7

-----------------------------Solution composition------------------------------

        Elements          Molality       Moles

        Al             3.217e-004  3.217e-004
        Ca             6.238e-004  6.238e-004
        Cu             2.486e-005  2.486e-005
        Fe             9.669e-007  9.669e-007
        K              1.023e-005  1.023e-005
        Mg             3.291e-004  3.291e-004
        N              1.428e-006  1.428e-006
        Na             1.740e-004  1.740e-004
        S(6)           1.884e-003  1.884e-003
        Si             1.947e-004  1.947e-004
        Zn             4.926e-005  4.926e-005

----------------------------Description of solution----------------------------

                                pH  =   4.800
                                pe  =   8.260
                    Activity of water  =   1.000
                      Ionic strength  =  5.543e-003
                     Mass of water (kg)  =  1.000e+000
                 Total alkalinity (eq/kg)  =  2.604e-005
                   Total carbon (mol/kg)  =  0.000e+000
                    Total CO2 (mol/kg)  =  0.000e+000
                  Temperature (deg C)  =  19.500
                Electrical balance (eq)  = -5.893e-004
 Percent error, 100*(Cat-|An|)/(Cat+|An|)  = -10.53
                           Iterations  =   9
                             Total H  = 1.110133e+002
                             Total O  = 5.551458e+001
```

----------Saturation indices----------

Phase	SI	log IAP	log KT	
Al(OH)3(a)	-1.06	10.10	11.17	Al(OH)3
Albite	-4.91	-23.27	-18.36	NaAlSi3O8
Alunite	5.70	4.99	-0.71	KAl3(SO4)2(OH)6
Anhydrite	-2.01	-6.35	-4.34	CaSO4
Anorthite	-7.64	-27.51	-19.87	CaAl2Si2O8
Ca-Montmorillonite	2.61	-43.22	-45.83	Ca0.165Al2.33Si3.67O10(OH)2
Chalcedony	-0.09	-3.71	-3.62	SiO2
Chlorite(14A)	-31.80	38.67	70.47	Mg5Al2Si3O10(OH)8
Chrysotile	-22.56	10.33	32.90	Mg3Si2O5(OH)4
Fe(OH)3(a)	-1.61	3.29	4.89	Fe(OH)3
Gibbsite	1.68	10.10	8.42	Al(OH)3
Goethite	4.09	3.29	-0.80	FeOOH
Gypsum	-1.77	-6.35	-4.58	CaSO4:2H2O
H2(g)	-26.12	-29.25	-3.13	H2
H2O(g)	-1.65	-0.00	1.65	H2O
Hematite	10.15	6.57	-3.58	Fe2O3
Illite	-0.86	-41.88	-41.02	K0.6Mg0.25Al2.3Si3.5O10(OH)2
Jarosite-K	-6.68	-15.46	-8.78	KFe3(SO4)2(OH)6
K-feldspar	-3.51	-24.50	-21.00	KAlSi3O8
K-mica	5.43	18.95	13.52	KAl3Si3O10(OH)2
Kaolinite	4.87	12.79	7.92	Al2Si2O5(OH)4
Melanterite	-6.89	-9.17	-2.28	FeSO4:7H2O
N2(g)	-2.90	-6.15	-3.24	N2
NH3(g)	-37.59	-35.71	1.88	NH3
O2(g)	-32.85	-35.70	-2.85	O2
Quartz	0.35	-3.71	-4.06	SiO2
Sepiolite	-15.20	0.71	15.91	Mg2Si3O7.5OH:3H2O
Sepiolite(d)	-17.95	0.71	18.66	Mg2Si3O7.5OH:3H2O
SiO2(a)	-0.95	-3.71	-2.76	SiO2
Talc	-19.12	2.91	22.04	Mg3Si4O10(OH)2
Willemite	-9.33	6.46	15.79	Zn2SiO4
Zn(OH)2(e)	-6.42	5.08	11.50	Zn(OH)2

End of simulation.

Reading input data for simulation 2.

End of run.

```
DATABASE C:\Program Files\USGS\Phreeqc Interactive 2.13.2\phreeqc.dat
        SOLUTION 1 LLBC-8
           temp      18.8
           pH        4.8
           pe        8.47
           redox     pe
           units     mg/kgw
           density   1
           Alkalinity 0
           N         0.11
           S(6)      183
           Cl        0
           Al        9010 ug/kgw
           Ca        26
           Cu        1640 ug/kgw
           Fe        67 ug/kgw
           Mg        8
           K         0.4
           Si        11.7
           Na        4
           Zn        3260 ug/kgw
           water     1 # kg
-------------------------------------------
Beginning of initial solution calculations.
-------------------------------------------

Initial solution 1.       LLBC-8

-----------------------------Solution composition------------------------------

        Elements          Molality       Moles

        Al              3.339e-004  3.339e-004
        Ca              6.487e-004  6.487e-004
        Cu              2.581e-005  2.581e-005
        Fe              1.200e-006  1.200e-006
        K               1.023e-005  1.023e-005
        Mg              3.291e-004  3.291e-004
        N               7.853e-006  7.853e-006
        Na              1.740e-004  1.740e-004
        S(6)            1.905e-003  1.905e-003
        Si              1.947e-004  1.947e-004
        Zn              4.987e-005  4.987e-005
```

----------Description of solution----------

pH = 4.800
pe = 8.470
Activity of water = 1.000
Ionic strength = 5.637e-003
Mass of water (kg) = 1.000e+000
Total alkalinity (eq/kg) = 2.512e-005
Total carbon (mol/kg) = 0.000e+000
Total CO2 (mol/kg) = 0.000e+000
Temperature (deg C) = 18.800
Electrical balance (eq) = -5.399e-004
Percent error, 100*(Cat-|An|)/(Cat+|An|) = -9.49
Iterations = 7
Total H = 1.110133e+002
Total O = 5.551466e+001

----------Saturation indices----------

Phase	SI	log IAP	log KT	
Al(OH)3(a)	-1.09	10.12	11.21	Al(OH)3
Albite	-4.92	-23.33	-18.41	NaAlSi3O8
Alunite	5.67	5.05	-0.62	KAl3(SO4)2(OH)6
Anhydrite	-1.99	-6.33	-4.34	CaSO4
Anorthite	-7.71	-27.61	-19.89	CaAl2Si2O8
Ca-Montmorillonite	2.59	-43.35	-45.94	Ca0.165Al2.33Si3.67O10(OH)2
Chalcedony	-0.09	-3.71	-3.62	SiO2
Chlorite(14A)	-32.03	38.71	70.74	Mg5Al2Si3O10(OH)8
Chrysotile	-22.65	10.33	32.99	Mg3Si2O5(OH)4
Fe(OH)3(a)	-1.33	3.56	4.89	Fe(OH)3
Gibbsite	1.66	10.12	8.46	Al(OH)3
Goethite	4.34	3.56	-0.77	FeOOH
Gypsum	-1.75	-6.33	-4.58	CaSO4:2H2O
H2(g)	-26.54	-29.66	-3.12	H2
H2O(g)	-1.67	-0.00	1.67	H2O
Hematite	10.65	7.13	-3.53	Fe2O3
Illite	-0.89	-42.01	-41.12	K0.6Mg0.25Al2.3Si3.5O10(OH)2
Jarosite-K	-5.90	-14.63	-8.72	KFe3(SO4)2(OH)6
K-feldspar	-3.51	-24.56	-21.05	KAlSi3O8
K-mica	5.39	19.01	13.63	KAl3Si3O10(OH)2
Kaolinite	4.84	12.83	7.98	Al2Si2O5(OH)4
Melanterite	-6.79	-9.08	-2.29	FeSO4:7H2O
N2(g)	-2.17	-5.41	-3.24	N2
NH3(g)	-37.83	-35.93	1.90	NH3
O2(g)	-32.25	-35.10	-2.84	O2

```
        Quartz           0.36   -3.71   -4.07  SiO2
        Sepiolite      -15.22    0.71   15.93  Mg2Si3O7.5OH:3H2O
        Sepiolite(d)   -17.95    0.71   18.66  Mg2Si3O7.5OH:3H2O
        SiO2(a)         -0.95   -3.71   -2.76  SiO2
        Talc           -19.21    2.91   22.12  Mg3Si4O10(OH)2
        Willemite       -9.38    6.47   15.85  Zn2SiO4
        Zn(OH)2(e)      -6.41    5.09   11.50  Zn(OH)2

------------------
End of simulation.
------------------
------------------------------------
Reading input data for simulation 2.
------------------------------------
-----------
End of run.
-----------


DATABASE C:\Program Files\USGS\Phreeqc Interactive 2.13.2\phreeqc.dat
        SOLUTION 1 LLBC-9
          temp      18.4
          pH        4.7
          pe        8.7
          redox     pe
          units     mg/kgw
          density   1
          Cl        0
          N         0.02
          S(6)      188
          Alkalinity 0
          Al        8990 ug/kgw
          Ca        26
          Cu        1630 ug/kgw
          Fe        65 ug/kgw
          Mg        8
          K         0.3
          Si        11.9
          Na        4
          Zn        3340 ug/kgw
          water     1 # kg
-------------------------------------------
Beginning of initial solution calculations.
-------------------------------------------

Initial solution 1.       LLBC-9
```

----------Solution composition----------

Elements	Molality	Moles
Al	3.332e-004	3.332e-004
Ca	6.487e-004	6.487e-004
Cu	2.565e-005	2.565e-005
Fe	1.164e-006	1.164e-006
K	7.672e-006	7.672e-006
Mg	3.291e-004	3.291e-004
N	1.428e-006	1.428e-006
Na	1.740e-004	1.740e-004
S(6)	1.957e-003	1.957e-003
Si	1.981e-004	1.981e-004
Zn	5.109e-005	5.109e-005

----------Description of solution----------

pH = 4.700
pe = 8.700
Activity of water = 1.000
Ionic strength = 5.716e-003
Mass of water (kg) = 1.000e+000
Total alkalinity (eq/kg) = 8.285e-006
Total carbon (mol/kg) = 0.000e+000
Total CO2 (mol/kg) = 0.000e+000
Temperature (deg C) = 18.400
Electrical balance (eq) = -6.299e-004
Percent error, 100*(Cat-|An|)/(Cat+|An|) = -10.92
Iterations = 8
Total H = 1.110133e+002
Total O = 5.551487e+001

----------Saturation indices----------

Phase	SI	log IAP	log KT	
Al(OH)3(a)	-1.41	9.83	11.24	Al(OH)3
Albite	-5.31	-23.74	-18.43	NaAlSi3O8
Alunite	4.93	4.37	-0.57	KAl3(SO4)2(OH)6
Anhydrite	-1.98	-6.32	-4.34	CaSO4
Anorthite	-8.57	-28.47	-19.91	CaAl2Si2O8
Ca-Montmorillonite	1.85	-44.14	-46.00	Ca0.165Al2.33Si3.67O10(OH)2
Chalcedony	-0.07	-3.70	-3.63	SiO2
Chlorite(14A)	-33.76	37.13	70.89	Mg5Al2Si3O10(OH)8

```
        Chrysotile      -23.29    9.74   33.04  Mg3Si2O5(OH)4
        Fe(OH)3(a)       -1.42    3.47    4.89  Fe(OH)3
        Gibbsite          1.34    9.83    8.49  Al(OH)3
        Goethite          4.23    3.47   -0.76  FeOOH
        Gypsum           -1.74   -6.32   -4.58  CaSO4:2H2O
        H2(g)           -26.80  -29.92   -3.12  H2
        H2O(g)           -1.68   -0.00    1.68  H2O
        Hematite         10.43    6.93   -3.50  Fe2O3
        Illite          -1.77  -42.94  -41.17  K0.6Mg0.25Al2.3Si3.5O10(OH)2
        Jarosite-K       -6.03  -14.72   -8.69  KFe3(SO4)2(OH)6
        K-feldspar       -4.02  -25.10  -21.08  KAlSi3O8
        K-mica            4.24   17.93   13.69  KAl3Si3O10(OH)2
        Kaolinite         4.23   12.25    8.02  Al2Si2O5(OH)4
        Melanterite      -6.79   -9.09   -2.29  FeSO4:7H2O
        N2(g)            -2.91   -6.15   -3.24  N2
        NH3(g)           -38.58  -36.67    1.91  NH3
        O2(g)           -31.88  -34.72   -2.84  O2
        Quartz            0.38   -3.70   -4.08  SiO2
        Sepiolite        -15.61    0.33   15.94  Mg2Si3O7.5OH:3H2O
        Sepiolite(d)     -18.33    0.33   18.66  Mg2Si3O7.5OH:3H2O
        SiO2(a)          -0.94   -3.70   -2.77  SiO2
        Talc            -19.83    2.34   22.17  Mg3Si4O10(OH)2
        Willemite        -9.79    6.09   15.88  Zn2SiO4
        Zn(OH)2(e)       -6.60    4.90   11.50  Zn(OH)2
------------------
End of simulation.
------------------
-----------------------------------
Reading input data for simulation 2.
-----------------------------------

-----------
End of run.
-----------
```